Running title: Fluvial-to-tidal transition in a mixed influenced delta

Fluvial-to-tidal transition in proximal, mixed tide- and wave-influenced deltaic deposits: Cretaceous lower Sego Sandstone, Utah, USA

Marijn van Cappelle[1,*], Stephen Stukins[2], Gary J. Hampson[1] and Howard D. Johnson[1]

[1]*Department of Earth Science and Engineering, Imperial College London, Royal School of Mines, Prince Consort Road, London, SW7 2BP, United Kingdom*

[2]*Department of Earth Sciences, Natural History Museum, Cromwell Road, London, SW7 5BD, United Kingdom*

**corresponding author: m.van-cappelle12@imperial.ac.uk*

Abstract

Facies models for regressive, tide-influenced deltaic systems are under-represented in the literature compared with their fluvial- and wave- dominated counterparts. Here a facies model is presented of the mixed, tide- and wave-influenced deltaic strata of the Sego Sandstone, which was deposited in the Western Interior Seaway of North America during the Late Cretaceous. Previous work on the Sego Sandstone has focused on the medial to distal parts of the outcrop belt where tides and waves interact. This study focuses on the proximal outcrop belt, in which fluvial and tidal processes interact. Five facies associations are recognized. Bioturbated mudstones (FA1) were deposited in an offshore environment and are gradationally overlain by hummocky cross-stratified sandstones (FA2) deposited in a wave-dominated lower shoreface environment. These facies associations are erosionally overlain by tide-dominated cross-bedded sandstones (FA4) interbedded with ripple cross-laminated heterolithic sandstones (FA3) and channelised mudstones (FA5). Palaeocurrent

directions derived from cross-bedding indicate bidirectional currents which are flood-dominated in the lower part of the studied interval and become increasingly ebb-/fluvial-directed upwards. At the top of the succession, ebb-/fluvial-dominated, high relief, narrow channel forms are present, which are interpreted as distributary channels. When distributary channels are abandoned they effectively become estuaries with landward sediment transport and fining trends. These estuaries have sandstones of FA4 at their mouth and fine landward through heterolithic sandstones of FA3 to channelised mudstones of FA5. Therefore the complex distribution of relatively mud- and sand-rich deposits in the tide-dominated part of the lower Sego Sandstone is attributed to the avulsion history of active fluvial distributaries, in response to a subtly expressed allogenic change in sediment supply and relative sea-level controls and autocyclic delta lobe abandonment.

Key-words: Sego Sandstone, facies architecture, fluvial-to-tidal transition, mixed influenced delta, tides, waves

1. Introduction

Tide-dominated deltaic deposits are the result of a complex interplay of depositional processes, which change from proximal to distal locations along the axes of distributary channels and onto the delta front. Fluvial processes dominate in landward locations, but these increasingly interact with tides in a coast-normal orientation, along the landward to seaward sediment transport path (Plink-Björklund, 2005; Van den Berg et al., 2007; Salahuddin & Lambiase, 2013). The changing balance of fluvial and tidal processes causes predictable variations in hydrodynamic energy, grain size, sand-mud ratio and facies types (Dalrymple & Choi, 2007). Wave reworking at the coastline may further complicate the depositional systems, for example via along-shore redistribution of sediment (Legler et al., 2014). The relative strength and interplay of these riverine, tidal and wave-driven depositional processes exerts a primary control on the dimensions, geometry, orientation and distribution of sediment bodies and facies belts in the geological record (Ainsworth et al., 2011).

Most ancient tide-influenced and tide-dominated deposits are interpreted to be deposited along transgressive coastlines. Many of the depositional models of these ancient transgressive tide-influenced systems (e.g. Yoshida et al., 2001; Yoshida et al., 2004; Plink-Björklund, 2005; Dalrymple, 2006; Sixsmith et al., 2008; Pontén & Plink-Björklund, 2009) are based on early work on well-studied modern estuaries and barrier-back barrier systems in high latitudes which developed during the Holocene transgression (e.g. Van Straaten & Kuenen, 1957; Oomkes & Terwindt, 1960; Van Straaten, 1961; Evans, 1965; Reineck, 1967; Terwindt, 1971). Detached tidal ridges are interpreted in many ancient transgressive shelf mudstone successions, consistent with early work on modern analogues (e.g. Houbolt, 1968; Boyles & Scott, 1982; Tillman & Martinsen, 1984; Gaynor & Swift, 1988; Olariu et al., 2012; Zhuo et al., 2014). A second line of approach to interpret tide-influenced deposits uses sequence stratigraphic models in which they are interpreted to be deposited in incised valleys during transgressions (e.g. Dalrymple, 1992; Dalrymple et al., 1992; Posamentier & Allen, 1999). A common feature for tide-dominated deposits in both types of interpretation mentioned above is that they form in transgressive settings, although we know from modern examples that many prograding tide-influenced and tide-dominated deltaic systems also exist. In particular, large modern tide-dominated river deltas in the tropics have been studied in detail (e.g. Harris et al., 1993; Allen & Chambers, 1998; Ta et al., 2002; Dalrymple et al., 2003; Hasan Sidi et al., 2003). However, prograding tide-dominated (Yang & Nio, 1989; Maguregui & Tyler, 1991; Martinius et al., 2001; McIlroy et al., 2005; Tänavsuu-Milkeviciene & Plink-Björklund, 2009; Legler et al., 2013; Chen et al., 2014), mixed tide-fluvial influenced (Pontén & Plink-Björklund, 2007) and mixed tide-wave influenced (Willis et al., 1999; Mellere & Steel, 2000; Willis & Gabel, 2001; Seidler & Steel, 2001) deltaic systems are not interpreted frequently in ancient strata. Facies architecture and stratigraphic relationships have been documented in several ancient tide-influenced or tide-dominated deltas. However, the facies architecture of the area where fluvial and tidal processes interact has yet to be characterised in such deltaic deposits, while this fluvial- to tidal transition is widely recognized in corresponding transgressive systems (e.g. Dalrymple et al., 1992; Plink-Björklund, 2005).

In order to develop a sound understanding of the facies relationships and stratigraphic architectures resulting from the interaction of fluvial and tidal processes, well-documented outcrop examples are needed in which vertical and lateral facies dimensions and spatial relationships can be measured. One such outcrop dataset is provided by the Late Cretaceous lower Sego Sandstone, which is exposed in the almost continuous Book Cliffs (Utah and Colorado, USA) over a distance of c. 150 km (e.g. Young, 1955). Overall the Sego Sandstone in this area is widely interpreted as an ancient tide-dominated or tide-influenced delta complex, because it records a succession of nearshore sandstones bearing a suite of tidal structures, which prograded over marine mudstones and which are overlain by non-marine deposits (e.g. Young, 1955; Willis & Gabel, 2001; Legler et al., 2014). This interpretation includes subordinate components of the lower Sego Sandstone, which are considered to be estuarine (Van Wagoner, 1991; Willis, 2000). The central and eastern parts of the outcrop belt, which contain medial to distal deltaic deposits in which tidal and wave processes interacted, have been extensively documented in detail in previous studies (Van Wagoner, 1991; Willis & Gabel, 2001; Willis & Gabel, 2003; Wood, 2004; Burton & Wood, 2011; Legler et al., 2014). In contrast, more proximal deposits in the western part of the outcrop belt have been described to date only in large, regional studies (Yoshida et al., 1996; Willis, 2000; McLaurin & Steel, 2000; Hettinger & Kirschbaum, 2002; Aschoff & Steel, 2011a). In this paper, we aim to develop an improved understanding of the proximal deposits of the Sego Sandstone, in which fluvial and tidal processes interacted. This aim is achieved by documenting facies characteristics within a framework of carefully traced stratigraphic surfaces and architectural elements in the part of the Sego Sandstone outcrop belt that has previously only been covered by regional studies.

2. Geological setting

The Sego Sandstone is part of the Mesaverde Group, which was deposited during the Campanian (Late Cretaceous) in the foreland of the North American Cordillera. To the west, the Farallon Plate was being subducted below the North American continent, resulting in the formation of a magmatic

arc and the thin-skinned Sevier Orogen fold-and-thrust-belt. A combination of flexural subsidence due to loading of the orogen and dynamic subsidence due to subduction of the cold Farallon Plate slab below the continent resulted in the creation of a wide basin in the centre of the North American continent (DeCelles, 2004; Liu & Nummedal, 2004; Liu et al., 2014). This wide basin was eventually flooded to form the Western Interior Seaway (Fig. 1A). Sediment was transported from the Sevier Orogen eastward into the Western Interior Seaway to deposit a series of clastic coastal sediment wedges, which record repeated shoreline progradation and retrogradation (e.g. Young, 1955).

The Sego Sandstone forms part of the progradational component of one such wedge (Fig. 2) and has a duration of about 2.5 Myr (Gill & Hail, 1975; Cobban et al., 2006). It overlies the marine Buck Tongue of the Mancos Shale and is overlain by coal-bearing, lower coastal plain deposits of the Neslen Formation. The Sego Sandstone is informally sub-divided into lower and upper intervals that are separated by the marine Anchor Mine Tongue of the Mancos Shale. Towards the east, both intervals of the Sego Sandstone pass into the Mancos Shale (Young, 1955). Towards the west, the Sego Sandstone correlates with the middle, relatively mudstone-rich part of the Castlegate Sandstone (Yoshida et al., 1996; McLaurin & Steel, 2000; Willis, 2000; Aschoff & Steel, 2011a).

The lower Sego Sandstone crops out in a 150 km long outcrop belt in the Book Cliffs between the towns of Green River, Utah, and Grand Junction, Colorado (Fig. 1B). The central portion of this outcrop belt is oriented SW-NE, parallel to the interpreted palaeo-coastline trend (i.e. along depositional strike). In this central area, the lower Sego Sandstone consists of offshore mudstones, storm-generated hummocky cross-stratified (HCS) sandstones, and heterolithic sandstones with a strong tidal signature (Van Wagoner, 1991; Willis & Gabel, 2001; Willis & Gabel, 2003; Wood, 2004; Burton & Wood, 2011). Tidal deposits are erosionally based, with either tabular or lenticular geometries. Originally, such tidal sand bodies were interpreted as the infill of incised valleys, with their erosional bases defining nine sequence boundaries (Van Wagoner, 1991; Yoshida et al., 1996; Willis, 2000). More recently, many of these erosion surfaces have been attributed to tidal scour

inherent in the formation, migration and abandonment of tide-influenced deltaic distributary channels (Willis & Gabel, 2001; Willis & Gabel, 2003). These latter authors have interpreted three regressive-transgressive tongues in the lower Sego Sandstone, each comprising (1) a coarsening-upward succession of offshore mudstones passing gradationally into hummocky cross-stratified sandstones, which are interpreted as wave-dominated shoreface deposits, and (2) an overlying, erosionally based unit comprising heterolithic tidal sandstones, which are interpreted as tidal bar and channel-fill sand bodies. The high-relief (up to 30 m) erosion surfaces that cut down from near the top of each upward-coarsening succession are interpreted as sequence boundaries (Willis & Gabel, 2003). The stratigraphic architecture of each regressive-transgressive tongue was interpreted to record a temporal change in process regime, with wave-dominated deposits assigned to an early highstand systems tract, and overlying tide-dominated deposits assigned to late highstand to lowstand systems tracts (Willis & Gabel, 2001). Transgressive deposits are limited to thin (<5 m) bioturbated sandstones at the top of each tongue.

The eastern part of the outcrop belt is a W-E-trending section, which is oriented oblique to depositional dip. In this section, the lower Sego Sandstone comprises erosionally based tidal sandstones that interfinger with, and pass eastward (offshore) into, wave-reworked sandstones. This relationship implies that waves and tides operated at the same time, at least in the proximal part of the delta front. In such settings, preservation bias may result in the stratigraphic partitioning of tide- and wave-dominated deposits in shallower and deeper water environments, respectively (Legler et al., 2014).

The high relative influence of tides in the Sego Sandstone is unusual, in that underlying and overlying strata were deposited under a wave-dominated process regime (Aschoff & Steel, 2011b). High relative tidal influence has been attributed by some workers to deposition in a broad embayment ("Utah Bight") during tectonic reconfiguration of the basin, which resulted in a broad, shallow seafloor of irregular bathymetry (Steel et al., 2012).

3. Dataset and methods

Twenty-nine stratigraphic sections have been measured in a 25 km long, continuously exposed section of the Book Cliffs outcrop belt between Tusher Canyon and Crescent Canyon in east-central Utah (Fig. 1C). Strata in this area have a uniformly low (<5˚) tectonic dip towards the north. Stratigraphic logs are measured where canyons cut through the cliff face. In between the measured logs, stratal units have been traced in cliff faces using photo-panoramas.

Facies associations are identified based on lithology, sedimentary structures and ichnology, and are characterised and interpreted using facies analysis. Then the vertical stacking of facies associations in successions is defined and estimates for palaeo-water depth relative to effective storm- and fairweather-wave base are made in order to interpret sequence stratigraphic surfaces and the units that they bound. Lastly, the dimensions, geometries and lateral distributions of facies associations are characterised within the context of sequence stratigraphic units. This is achieved using 29 of the measured sections, with an average spacing of ~1km, and photo-panoramas of the intervening cliff exposures. The resulting architectural interpretations therefore follow the rugose map-view pattern of the Sego Sandstone outcrops (Fig. 8).

In addition, eight samples that are representative of the sedimentological facies were processed and analysed for their palynological content, and their palynofacies are documented herein. Palynological studies have been rarely undertaken in the Book Cliffs (Oboh-Ikuenobe, 1996), but may provide important additional information for facies analysis of tide-influenced deltaic systems (Stukins et al., 2013). The samples were treated with concentrated hydrochloric acid (37%) where necessary to remove carbonate material and then treatment with hydrofluoric acid (40%) to remove silicates and leave an organic residue. All residues were sieved using a 15 µm polyester mesh and then mounted onto glass slides using a visible light curing mounting medium (Rapidslide).

4. Facies Associations

Five facies associations (FA) have been recognized based on observations of lithology, grain size and sorting, sedimentary structures, palaeocurrents, body fossils, and trace fossils. Bioturbation intensity is recorded using the bioturbation index (BI) scheme of Taylor & Goldring (1993). A summary of the facies association descriptions is given in Table 1. Palynofacies analysis was undertaken using a simple count scheme of categories (Table 2), and a minimum of 300 particles were counted for each sample before normalising as a percentage. Other organic particles (e.g. fungal remains, monolete spores) that do not appear in Table 2 were not encountered in the palynofacies count. One sample (FA4-1) was barren of any discernible organic residue. Analysis of the palynofacies data used concepts from Traverse (1994) and Tyson (1995).

4.1. Facies Association 1: Bioturbated mudstones

Description

FA1 consists of dark grey to rarely black homogenous claystones that grade into silty claystones, mudstones and pale yellow siltstones. In the claystones and mudstones, thin (<10 cm) siltstone and very fine-grained sandstone beds with sharp or gradational boundaries are present (Fig. 3A). Some siltstone beds contain low-angle cross-lamination and have a sharp lower boundary and a gradational, sharp or symmetrically rippled top. Lenticular siltstone-mudstone alternations and wavy siltstone-mudstone alternations are present locally. Bioturbation is generally low to moderate in intensity (BI of 2-3), but is locally absent (BI of 0) and high (BI of 4). Trace fossils include *Palaeophycus*, *Planolites*, *Schaubcylindrichnus*, *Thalassinoides*, *Skolithos* and *Arenicolites*, which in combination constitute the Cruziana ichnofacies (MacEachern & Bann, 2008).

The palynofacies of FA1 is characterised by a dominance of translucent phytoclasts (67-74%) and the lowest assemblage percentage for cuticle material. There are no marine palynomorphs (dinoflagellates or foraminiferal test linings) or Amorphous Organic Matter (AOM) within the count, but pollen and spores are present.

Interpretation

The fine grain size and occurrence of the Cruziana ichnofacies indicate deposition in a quiet, open-marine environment below effective storm-wave base (MacEachern & Bann, 2008). Siltstone and very fine-grained beds indicate episodic transport of coarser-grained sediment, probably during high river discharge and/or storm events (Wright, 1977; Bhattacharya & MacEachern, 2009). Although identified by the ichnofabric as marine, there are no marine palynomorphs in the palynofacies count. This is most likely because the assemblage is dominated by phytoclasts that drown out values of other organic particles. Further qualitative examination of only the palynomorphs shows an abundant assemblage of dinoflagellate cysts and several specimen of foraminiferal test linings, therefore indicating that marine surface- and benthic conditions were present. The dominance of translucent phytoclasts in the palynofacies assemblage exceeds the presence of opaque phytoclasts, which is consistent with a deltaic environment that was relatively distal to any trunk channel system (Hart et al., 1994; Tyson, 1995). This facies association corresponds to the mudstone part of the "transgressive and highstand system tract facies" of Van Wagoner (1991), the mudstone part of facies C of Willis (2000), facies 1 of Willis & Gabel (2001) and to the bioturbated mudstone intervals of facies association 1 of Legler et al. (2014).

4.2. Facies Association 2: Hummocky cross stratified sandstones

Description

FA2 consists of thin (10-50 cm), tabular beds of very fine- and lower fine-grained sandstone. Individual beds can be traced laterally over distances of up to 1 km, and groups of beds can be traced over distances of up to 10 km. The beds have a sharp base and either a sharp, rippled or a gradational top. Internally the beds contain HCS with a wavelength of 0.5-2m and a preserved bed thickness of 10-50 cm (Fig 3B). Bioturbation is generally absent to low in intensity (BI of 0-2). Trace fossils include *Skolithos*, *Palaeophycus*, *Ophiomorpha*, *Planolites*, *Arenicolites* and *Diplocraterion*, constituting a mixture of the Cruziana and Skolithos ichnofacies (MacEachern & Bann, 2008). The

sandstone beds alternate with bioturbated mudstones of FA1. In general, FA2 gradationally overlies FA1, and occurs in coarsening-upward successions in which sandstone beds are increasingly erosionally amalgamated towards the top. This FA is overlain by bioturbated mudstones of FA1 or is erosionally overlain by cross-bedded sandstones of FA4.

Interpretation

The presence of sandstone beds displaying HCS indicates deposition by episodic storm events in water depths between the effective storm wave base and fairweather-wave base (Dott & Bourgeois, 1982; Duke, 1985; Keen et al., 2012). This interpretation is supported by the occurrence of a mixed Cruziana and Skolithos ichnofacies (MacEachern & Bann, 2008). The upward increase in the abundance and amalgamation of storm-event beds indicates that storms became more frequent towards the top of the succession, due to an increasingly energetic wave climate and/or progressive shallowing of water depth (Storms & Hampson, 2005). This facies association corresponds with the "transgressive and highstand system tract facies" of Van Wagoner (1991), facies C of Willis (2000), facies 2 of Willis & Gabel (2001) and with intervals of HCS sandstone interbedded with bioturbated mudstones in facies associations 1 and 2 of Legler et al. (2014).

4.3. Facies Association 3: Ripple cross-laminated heterolithic sandstones

Description

This facies association consists of very fine- to fine-grained sandstones and mudstones that exhibit flaser, wavy and lenticular bedding (Reineck & Wunderlich, 1968). The sandstone-to-mudstone ratio in the facies association is 0.5-0.9. Ripple cross-lamination and both symmetrical and asymmetrical rippled surfaces are present (Fig. 4A, B, D). Asymmetrical ripples with bedform heights of 1-2 cm and wavelengths of 5-10 cm display apparent bidirectional palaeocurrent patterns. Along individual rippled surfaces, lateral changes from asymmetrical to symmetrical ripples occur. Up to centimetre-scale mudstone clasts are common. Coal fragments up to 1 cm in diameter and carbonaceous mudstone drapes are also present. Bioturbation is generally absent to low in intensity (BI of 0-2), and

trace fossils include *Ophiomorpha*, *Thalassinoides*, *Skolithos*, *Planolites*, *Palaeophycus* and *Gyrochorte* (Fig. 4C). The trace fossil assemblage constitutes an impoverished, mixed Cruziana and Skolithos ichnofacies (MacEachern & Bann, 2008). This facies association alternates with cross-bedded sandstones of FA4. In these alternations, the lower boundary of FA3 is marked by a sharp decrease in sandstone grain size and an increase in mudstone content. The upper contact of FA3 is defined by the erosional base of FA4. Towards the top of the lower Sego Sandstone, FA3 is deposited above or below FA5, and contacts between the two facies associations are sharp.

There is a variable palynofacies characterisation for FA3, however there is consistently a relatively high percentage of cuticle material in all samples. The highest numbers of dinoflagellate cysts and resin are present in palynofacies counts from FA3 samples. Phytoclasts are the dominant organic particle. The type of phytoclast however, is not consistent. The samples containing the dinoflagellate cysts within the palynofacies count have a far higher proportion of translucent phytoclast than the samples, which lack dinoflagellate cysts and contain a greater proportion of equidimensional, opaque phytoclasts.

Interpretation

The abundance of asymmetrical ripple forms and current ripple cross-lamination indicate that sand was predominantly deposited as ripples migrating in response to unidirectional subaqueous currents. The occurrence of symmetrical ripple forms also shows that oscillatory waves were dominant episodically. The interbedding of sandstone and mudstone beds indicates temporal changes in current velocities. The resulting heterolithic facies contain apparent bidirectional palaeocurrents, which supports deposition by tidal processes (Oomkes & Terwindt, 1960; Reineck & Wunderlich, 1968; Terwindt, 1971; Van den Berg et al., 2007). The tidal reworking of the sediment on a daily basis suggests deposition above fairweather wave base. The low intensity of bioturbation by an impoverished Cruziana and Skolithos ichnofacies is consistent with deposition in a stressed environment characterised by fluctuating energy levels, a mobile sediment substrate and/or

restricted marine salinities (MacEachern & Bann, 2008). The heterolithic nature of this facies association is reflected in the palynofacies values. The higher percentage of cuticle material in samples of FA3 than those of FA1, may indicate a closer proximity to a significant sediment fairway (Hart et al., 1994; Tyson, 1995). The greater ratio of equidimensional to bladed opaque phytoclasts corroborates this conclusion. Samples of FA3 also contain a greater percentage of opaque phytoclasts that were most likely deposited in association with a proximal supply of terrestrial sediment. This facies association corresponds with the thinly bedded, finer grained part of the "lowstand system tract facies" of Van Wagoner (1991) and facies 3 of Willis & Gabel (2001).

4.4. Facies Association 4: Cross-bedded sandstones

Description

Facies association 4 occurs in units with sharp, planar to erosional bases that are locally lined by wood debris, mudstone clasts and rare shell debris (Fig. 5C). Above the basal surface, trough cross-bedded, fine- to medium-grained sandstones are present, marking an abrupt increase in grain size compared to the underlying very fine- to fine-grained sandstones of FA2 or FA3. Trough cross-beds occur in sets that are generally 20-40 cm thick. Sets are stacked into cosets that occur in sandstone beds defined by a sharp erosional base and with a top marked by abrupt fining in grain size or by a sharp erosional contact at the base of the overlying unit. In such beds, cross-sets indicate unidirectional palaeocurrents with a large spread of c. 90°. Locally, bidirectional palaeocurrents in cosets are observed. The sandstones may be devoid of finer grained material, but commonly contain variable amounts of mudstone drapes, carbonaceous mudstone drapes, mudstone flasers and mudstone clasts. Mudstone drapes line foresets, which merge and thicken down-dip into mudstone and sometimes rippled heterolithic toesets (Fig. 5A, B). Units of this sandstone-dominated facies (>90% sand) contain internal low-angle (generally 5° and up to 10°) accretion surfaces dipping towards the NE and SW, but other dip directions occur as well. Coaly clasts and wood debris are sparse and are bored by rare *Teredolites*. Bioturbation is generally absent (BI of 0), but sparse

296 bioturbation (BI of 1-2) is locally present. Trace fossils are dominated by *Ophiomorpha* and *Skolithos*,
297 but also include *Palaeophycus*, *Planolites*, *Gyrochorte*, *Arenicolites*, *Rosellia* and *Cylindrichnus*. This
298 assemblage constitutes a mixture of the Cruziana and Skolithos ichnofacies (MacEachern & Bann,
299 2008). The top of FA4 is often free of mudstone, it is usually completely reworked by *Ophiomorpha*
300 and less commonly by *Skolithos* (BI of 5-6) (Fig. 5D), and contains spherical red concretions (up to c.
301 50 cm in diameter).

302 **Interpretation**

303 The prevalence of cross-bedding indicates deposition from subaqueous dunes that migrated in
304 response to relatively strong currents. The geometry, abundance and distribution of mudstone
305 drapes are typical of those generated by tidal currents above fairweather wave base, which fluctuate
306 on a daily basis (Allen, 1980; Visser, 1980; Van den Berg et al., 2007). This interpretation is supported
307 by the presence of bidirectional palaeocurrents. Based on regional palaeogeographic considerations
308 (Willis & Gabel, 2001; Wood, 2004), palaeocurrents directed towards the NW are interpreted as
309 flood tidal currents and those directed towards the SE are interpreted as ebb and fluvial currents.
310 The low diversity of the trace fossil assemblage is consistent with deposition in a high-energy marine
311 environment, possibly with brackish water conditions. The sharp, lag-lined bases of units of FA4 are
312 interpreted as tidal erosion surfaces, possibly enhanced by fluvial discharge, at the base of tidal
313 channels. The cosets of inclined surfaces indicate dune migration across larger bar-forms. Where
314 units of FA4 exhibit planar, laterally continuous bases, inclined bedding may also indicate the
315 presence of highly mobile bar-forms. This interpretation indicates that multiple parallel bar forms
316 covered, and migrated in an area with a water depth at which tidal currents affected bed-load
317 transport in the form of subaqueous dunes (Houbolt, 1968; Harris et al., 1992; Trentesaux et al.,
318 1999). The abundance of wood debris, coal clasts and carbonaceous mudstone drapes indicates
319 nearby vegetated areas, consistent with an emergent deltaic to coastal plain setting. The intensely
320 bioturbated tops of units of FA4 indicate an increase in biogenic activity, probably associated with

reduced sedimentation following channel abandonment. This facies association corresponds with the coarser grained cross stratified part of the "lowstand system tract facies" of Van Wagoner (1991), facies D of Willis (2000), facies 4 and 5 of Willis & Gabel (2001) and facies associations 6 and 7 of Legler et al. (2014).

4.5. Facies Association 5: Sharp-based mudstones and heterolithic mudstones

Description

Facies association 5 consists of dark grey to black, carbonaceous mudstones. Very fine-grained sandstone is present in intervals of lenticular and wavy bedding (c. 0.1 to 10 cm thick). The sandstone-to-mudstone ratio of the facies association is 0-0.5. Units of FA5 have sharp concave-upward, erosional bases above which there is an upward increase in mudstone content (Fig. 6A, B). In some cases, sharp internal boundaries are present which are overlain by very fine grained sandstones that rapidly fine upwards into mudstones (Fig. 6C). Each unit is thus channelised, with a lateral extent of up to 1 km. Some internal bedding surfaces within channelised units of FA5 are inclined, and associated with abrupt lateral changes in sandstone-to-mudstone ratio (inclined heterolithic strata, IHS, *sensu* Thomas et al., 1987). Bioturbation is generally absent (BI of 0), with sparse *Planolites* present locally (BI of 1). The palynofacies for FA5 is very similar to that of FA1, however with the addition of dinoflagellate cysts and AOM (Amorphous Organic Matter) included in the count data.

Interpretation

The concave-upward erosional bases of units of FA5 record deposition in channels. The low sandstone-to-mudstone ratio of the facies association indicates deposition predominantly from suspension due to low flow velocities, high suspended sediment concentrations and/or a deficiency of sand supply. The occurrence of lenticular and wavy bedding signifies intermittent tidal current activity through the channels (Van Straaten & Kuenen, 1957; Oomkes, 1974; Staub & Gastaldo, 2003; Legler et al., 2013). Furthermore, IHS indicates accretion of a mobile substrate within laterally

346 migrating channels (Reineck, 1958; Thomas et al., 1987; Choi et al., 2004). The abundance of
347 carbonaceous organic material indicates that nearby vegetation was eroded by and transported
348 through the channels (Oomkes, 1974; Staub & Gastaldo, 2003). The near absence of bioturbation
349 indicates a highly stressed environment (MacEachern & Bann, 2008). FA5 is interpreted as the fills of
350 low-energy to inactive (abandoned) deltaic distributary channels in a shallow water environment on
351 the lower delta plain. It is likely that these channels retained an open connection with the sea during
352 abandonment, forming estuarine channels (Dalrymple et al., 1992). Abundant organic material is
353 inferred to have been derived from surrounding supra-tidal salt marshes on the lower delta plain.
354 The similarities of the palynofacies with FA1 indicate that the deposition was not directly connected
355 to a fluvial source, but is instead consistent with the deposition of fine grained material by tidal
356 currents within abandoned channels. Funnelling of more saline waters along abandoned tidal
357 channels can often extend the range of marine palynomorphs to potentially more proximal
358 locations, explaining the occurrence of dinoflagellate cysts and AOM (Amorphous Organic Matter) at
359 this position (Hubbard et al., 2011). This FA corresponds with facies A of Willis (2000).

360 ## 5. Facies successions

361 ### 5.1. Wave-dominated successions S_{-1} and S_0

362 Two upward-coarsening successions characterise the lower part of the studied interval, each
363 comprising FA1 gradationally overlain by FA2. The two facies successions extend across most of the
364 study area (Figs. 7, 8). The lower upward-coarsening succession is named S_{-1} by extending the
365 nomenclature of Willis & Gabel (2003) for the Sego Sandstone in exposures directly to the east of
366 the study area. It has a thickness of 3 to 11 m. The overlying upward-coarsening succession, S_0, has a
367 thickness of 3 to 18 m. The upward-coarsening trend in each succession may represent an increase
368 in storm energy, an increase in sand supply and/or an upward shallowing in palaeo-water depth
369 (Storms & Hampson, 2005; Sømme et al., 2008).

5.2. Mixed, wave- and tide-influenced succession S_1

A third upward-coarsening succession comprising FA1 and FA2 is erosionally overlain by cross-bedded sandstones of FA4 (sandstone S_1 after Willis & Gabel, 2001) across a laterally extensive, planar erosion surface (Fig. 7). It is interpreted that the facies succession of FA1, FA2 and FA4 is a genetic succession. The transition from FA2 to FA4 is attributed to an upward shallowing in palaeo-water depth from below to above the maximum depth to which currents scoured the sea bed when spring tides, storms and high fluvial discharge coincided to form the highest flow velocities. This scour depth is likely to have varied over different temporal scales, ranging from tidal cycles through to longer term periods, possibly seasonal, that could reflect periods when tidal currents were augmented by storm and river flood events. Spatial variations also occur due to fluctuations in the relative strength of tidal currents relative to wave-induced and river currents (Dalrymple & Choi, 2007; Legler et al., 2014). Alternatively, the erosion surface may record erosion during lowering of relative sea-level and forced regression (Willis & Gabel, 2001). The top of the facies succession is marked by an abrupt upward fining across a sharp surface. This facies succession has a thickness between 8 and 18 m, with an average of 13 m. The facies succession is present over the whole extent of the study area (Figs. 7, 8), and also in other parts of the Book Cliffs outcrop belt, where abrupt fining at the top of this facies succession marks a regionally correlative flooding surface (Van Wagoner, 1991; Willis & Gabel, 2003).

5.3. Tide-dominated successions S_2 and S_3

The upper part of the studied interval (sandstones S_2 and S_3 after Willis & Gabel, 2001; Figs. 7, 8) comprises alternations of FA3 and FA4, with FA5 also present locally. The architecture of these strata is complex, and varies laterally from east (palaeoseaward) to west (palaeolandward) (Figs. 7, 8), as described in the next section of the paper. Multiple upward-coarsening successions of variable thickness (1-10 m) consist of FA3 overlain by FA4 (Fig. 7). Each succession is characterized by: (1) an increase in grain size from very fine- to fine-grained sandstone, (2) an upward decrease in mudstone content, (3) an upward increase in sandstone bed thickness, and (4) an increase in the size of

sedimentary structures, from centimetre-scale ripple cross-lamination to decimetre-scale dune cross-bedding. Since both FA3 and FA4 were deposited principally by tidal currents, this part of the succession is considered to be tide-dominated. The presence of coal clasts and carbonaceous drapes may indicate erosion and transport on the lower delta plain during high river discharge, and therefore the indirect influence of fluvial processes. The tide-dominated deposits of S_2 and S_3 are 18-32 m thick, with an average of 25 m. A prominent sandstone (S_3) with a thickness of 1-15 m forms the uppermost part of the lower Sego Sandstone over most of the study area (Figs. 7, 8). It is interpreted that the deposits of FA3 and FA4 are deposited in the sub-tidal zone because no indications for subaerial exposure are observed (Van Straaten, 1961; Allen, 1980; Visser, 1980). The deposits of FA5 are interpreted to represent abandoned distributary channels in the inter-tidal zone, such that the presence of FA5 indicates an upward shallowing in palaeo-water depth (Van Straaten & Kuenen, 1957; Oomkes, 1974; Staub & Gastaldo, 2003). Also, the upper sandstone (S_3) has a high relief erosional surface at its base, which is interpreted to have been cut by distributary channels (as discussed in a later section). Distributary channels mark the shallowest palaeo-water depth in delta front successions (Li & Bhattacharya, 2014). Therefore the whole succession of the lower Sego Sandstone is interpreted to be a generally upward-shallowing succession from offshore mudstones to the inter-tidal zone. The absence of any evidence of subaerial exposure can be explained by deposition during a forced regression (Posamentier & Morris, 2000; Prince & Burgess, 2013) and/or by transgressive erosion (ravinement) at the base of the Anchor Mine Tongue.

5.4. Marine Anchor Mine Tongue

Marine mudstones (FA1) of the Anchor Mine Tongue define the top of the lower Sego Sandstone in the eastern part of the study area (east of Horse Mesa; Figs. 1C, 8). Farther west, the Anchor Mine Tongue passes into hummocky cross-stratified and intensely bioturbated sandstones (FA2 and FA4). The Anchor Mine Tongue records an increase in water depth across a regionally extensive flooding surface (Van Wagoner, 1991; Willis, 2000; Willis & Gabel, 2001; Hettinger & Kirschbaum, 2002; Aschoff & Steel, 2011a; Legler et al., 2014).

6. Stratigraphic architecture

The vertical facies successions described above can be traced laterally for kilometres to tens of kilometres throughout the study area (Figs. 1C, 8). In some of the cliff-face amphitheatres, 3D reconstruction of stratigraphic architecture and facies-association distributions over several hundreds of metres have been documented (Fig. 9). Palaeocurrent data from the various stratigraphic intervals, and their respective facies successions, provide extensive documentation of sediment transport directions along large tracts of the cliff-face outcrop belt (Fig. 10).

6.1. Wave-dominated successions S_{-1} and S_0

Upward-coarsening successions S_{-1} and S_0 exhibit minor lateral changes in thickness and have a uniform internal facies composition and relatively tabular geometries. Succession S_{-1} has a thickness of at least 14 m. Hummocky cross-stratified, lower shoreface sandstones (FA2) of succession S_{-1} are 2-3 m thick in the central the central part of the study area (logs 10-13, around Horse Mesa; Figs. 1C, 8), and pinch out laterally towards the west and east. Succession S_0 is 3-6 m thick, of which the upper 1-2 m comprises lower shoreface sandstones (FA2) where it overlies succession S_{-1} in the Horse Mesa area (logs 10-13, Fig. 8). Towards the west, the thickness of succession S_0 decreases to 3 m and the lower shoreface sandstones pinch out. Towards the east, where succession S_{-1} is absent, succession S_0 thickens to more than 18 m, with lower shoreface sandstones comprising the upper 9 m.

The regional coastline was oriented NE to SW (Willis & Gabel, 2001; Wood, 2004). Therefore it is interpreted that succession S_{-1} represents southeastwards progradation. The eastern (palaeoseaward) limit of lower shoreface sandstones (FA2) lies just east of Horse Mesa (log 13, Fig. 8). During subsequent southeastward progradation, which resulted in deposition of succession S_0, lower shoreface sandstones (FA2) extended across the entire study area. The thickening of succession S_0 on the flanks of laterally discontinuous lower shoreface sandstones (FA2) in succession S_{-1} (Fig. 8) implies infilling of depositional topography developed at the top of succession S_{-1}. These

447 thickness patterns imply lateral shifting of depocentres between successions S_{-1} and S_0, which may
448 reflect compensational stacking of delta lobes.

449 6.2. Mixed, wave- and tide-influenced succession S_1

450 Upward-coarsening succession S_1 is 8-18 m thick in the study area, averaging 13 m (Fig. 8). The
451 facies-association components display irregular lateral variations in thickness, but average 5 m for
452 FA1, 5 m for FA2 and 4 m for FA4 (Fig. 8). These three FAs are interpreted to form one genetic
453 upward-coarsening succession of mixed wave- and tide-influenced deposition. Palaeocurrent
454 directions derived from cross-bedding in FA4 are multi-directional, with a dominant direction
455 towards the NW and subordinate directions towards the SE and NE (Fig. 10E). In the context of the
456 NE-SW-oriented palaeoshoreline (Fig. 1B; Willis & Gabel, 2003; Wood, 2004), the dominant NW-
457 ward direction is attributed to flood-tidal currents, and the subordinate SE-ward direction to fluvial
458 and ebb-tidal currents. NE-directed palaeocurrents may be attributed to local wave-driven longshore
459 drift, which could have deflected deltaic distributary and tidal channels, although the regional
460 longshore drift direction in the older Blackhaw Formation was directed towards the SW (Slingerland
461 & Keen, 1999; Hampson, 2010; Hampson et al., 2014). Alternatively, the NE-directed palaeocurrents
462 can be attributed to dunes that migrated obliquely over the complex morphology of nearshore tidal
463 bars (Houbolt, 1968). Intense bioturbation and abruptly decreasing grain size at the top of
464 succession S_1 (Figs. 7, 8) are attributed to a pronounced decrease in sedimentation rate, probably
465 related to rising relative sea-level. The same conditions occur at the top of succession S_1 to the east
466 of the study area (Fig. 1; Van Wagoner, 1991; Willis & Gabel, 2003), which supports this being a
467 regional flooding surface.

468 6.3. Tide-dominated succession S_2

469 There is an overall upward-coarsening trend from the top of succession S_1 towards the top of
470 succession S_3. This overall upward-coarsening trend is constructed via the vertical stacking of
471 multiple thin (1-10 m) upward-coarsening successions of tidal sandstones (FA3, FA4). In the east of

472 the study area (between logs 23 and 29, Floy Wash and Crescent Canyon in Fig. 1C), four such
473 upward-coarsening successions are generally present, although the number varies from three to
474 seven (Figs. 8, 9B). Within upward-coarsening successions there is lateral variability in mudstone
475 content between FA3 (10-50% mudstone) and FA4 (0-10% mudstone) (Fig. 9B). A typical succession
476 is characterised in its lower part by upward increases in grain size, sandstone content and sandstone
477 bed thickness in FA3 (Fig. 7). The upper parts of these successions are typically capped by low-relief,
478 nearly planar erosional surfaces overlain by blocky, cross-bedded sandstones of FA4 (Fig. 7). Further
479 west, between Floy Wash and Horse Mesa (between logs 10 and 23 in Fig. 1C), the upward-
480 coarsening successions display uniform thicknesses (5-15 m), tabular geometries and greater lateral
481 continuity (Fig. 8). Palaeocurrent directions are variable and lack clear trends (Fig. 10B-D). Inclined
482 surfaces within units of cross-bedded sandstones (FA4) are observed to dip towards the NE and SW
483 in locations where a 3D view in the cliffs is possible, while cross stratification shows SE and NW
484 directed palaeocurrents, which suggests that dune-scale bedforms migrated over bars which
485 accreted laterally between channels. Channelised mudstones (FA5) with a thickness of 1-5 m and a
486 width of less than 1 km wide are present in the upper half of this succession, except for two
487 examples in the lower half of this succession in stratigraphic log 20. The channelised mudstones
488 (FA5) are also more common in the western (more proximal) part of the outcrop belt between
489 stratigraphic logs 1 and 10, although they are present further east. In locations where individual
490 channels can be traced along curved cliff lines, it is observed that the long axes of the channels are
491 oriented roughly NW-SE (Figs. 8, 9A, C, 10G-I).

492 ### 6.4. Tide-dominated succession S_3

493 Channelised, cross-bedded sandstones (FA4) dominate interval S_3 to the north and north-west of
494 Horse Mesa (between logs 10 and 20 in Fig. 1C), where the basal erosion surface has up to 10 m of
495 relief (Fig. 9A). The largest channelised sandstone body in this stratigraphic interval is up to 15 m
496 thick. The tortuous outline of the outcrop belt north of Horse Mesa has enabled four WNW-ESE-
497 trending channels to be mapped (red lines numbered C1-C4 in Fig. 10F). Palaeocurrents in these

channelised sandbodies have a dominant SE-ward (fluvial and/or ebb-tidal) direction and a subordinate NW-ward (flood-tidal) direction.

7. Discussion

7.1. Depositional model for the proximal, lower Sego Sandstone

It is interpreted that the lower Sego Sandstone in the study area was deposited in a net-regressive, mixed tide- and wave- influenced deltaic environment. The upward-coarsening succession of FA1, FA2 and FA4 in interval S_1 is interpreted to represent upward shallowing and regression of genetically-linked facies tracts on a wave-dominated delta front. The abrupt change in grain-size across the planar erosion surfaces between FA2 and FA4 may record sediment bypass during erosion. The lateral continuity of the sandstone-rich and flood-current dominated interval S_1 indicates that mud was removed from the proximal delta front. This was probably caused by a combination of wave reworking (Legler et al., 2014) and strong tidal currents seaward of the turbidity maximum zone (Dalrymple & Choi, 2007). The wave reworking of the delta front is demonstrated by the prevalence of HCS (FA2), and provides a mechanism for transporting sand and mud alongshore into the mouths of inactive distributary channels (estuaries)(Fig. 11B).

In intervals S_2 and S_3, FA3, FA4 and FA5 interfinger laterally and vertically to form a tide-dominated facies-association complex that overlies the flooding surface above S_1. Tidal currents responsible for the cross-bedded sandstones (FA4) were concentrated through approximately coast-normal channel belts. Lateral migration of these channels, and their intimately associated tidal bars, is interpreted to have resulted in the development of extensive, low-relief scour surfaces. Upward-coarsening successions of FA3 and FA4 were deposited as tidal bars. Active and abandoned distributary channels are defined by sharp-based channelised successions of FA4 and FA5, respectively.

Palaeocurrent data from the tide-dominated deposits of FA3, FA4 and FA5 within interval S_1 display mainly onshore (flood-tidal) directions with subordinate offshore (ebb-tidal and/or fluvial) directions

(Fig. 10E). Palaeocurrent directions become more variable in interval S_2 (Fig. 10B-D). However, in the channelised sandstones in the upper part of interval S_3 there is a dominant offshore-directed (ebb-tidal and/or fluvial) trend, with a subordinate onshore-directed (flood-tidal) trend (Fig. 10A). The cross-bedded sandstones (FA4) with offshore-directed palaeocurrents that infill the high relief, but relatively narrow, channels in the upper part of interval S_3 are interpreted as fluvial-dominated, tide-influenced distributary channels. The S_2 interval displays more variable palaeocurrent patterns, although there is a higher proportion of onshore (flood-tide)-directed flows. Interval S_1 is dominated by onshore-directed palaeocurrents, implying local dominance of flood-tides. Flood-tidal currents that enter shallow estuarine channels from the ocean are subject to less friction, and thus attain higher velocities, than ebb-tidal currents. Therefore, in transgressive estuarine systems without a major contribution of river discharge to the ebb tide, the higher velocity flood tide transports much more sediment than the ebb tide, such that flood-directed palaeocurrent directions are likely to dominate in such settings (Johnson et al., 1982; Dronkers, 1986; Van der Spek, 1997). The lateral variability in palaeocurrent directions in the lower Sego Sandstone (Fig. 10A-E) can also be attributed to the presence of mutually evasive flood- and ebb-tidal channels. Mutually evasive channels are characteristic of tide-influenced coastlines (Ahnert, 1960; Harris, 1988; Dalrymple et al., 1990; Van Veen et al., 2005). These mutually evasive channels can be recognized in the ancient with the preservation of opposed current directions within separate tidal channel sandbodies, each displaying a superficially unidirectional trend (e.g. Legler et al., 2013). The presence of mutually evasive tidal channels can skew preserved palaeocurrent trends, especially in areas of limited outcrop distribution. However, the laterally extensive nature of the Sego Sandstone outcrops enables greater confidence to be placed in the depositional significance of the palaeocurrent trends.

Overall, the Sego Sandstone succession seems to preserve a temporal change that, from bottom to top, records an overall, net regressive, distal to proximal change: (1) onshore-directed currents dominated in estuary/distributary mouth settings (S_1), (2) bidirectional currents characterized intermediate/lower delta plain settings (S_2), and (3) offshore-directed currents (S_3) recorded the

548 combined dominance of fluvial and ebb-tidal currents in proximal estuarine/upper delta plain
549 locations. This is consistent with models developed for tide-dominated estuaries and deltas
550 (Dalrymple et al., 1992; Dalrymple et al., 2003; Harris et al., 2004; Dalrymple & Choi, 2007;
551 Salahuddin & Lambiase, 2013).

552 The occurrence and distribution of mud-rich facies (cross-laminated heterolithic sandstones of FA3
553 and mudstones and muddy heterolithic of FA5) may reflect two alternative, but not mutually
554 exclusive, mechanisms. Firstly, the preferred model for the distribution of the mud-rich facies is that
555 they represent the infill of the following types of channel: (1) abandoned channels, (2) less active,
556 relatively low-energy distributary channels, or (3) smaller, laterally-migrating tidal channels without
557 any updip fluvial connection (i.e. tidal channels that drain lower delta plain/outer estuarine areas,
558 including intertidal areas). In this model, FA3 may have been deposited in relatively medial locations,
559 near the widened, funnel-shaped mouths of less active and/or smaller channels in which sands of
560 FA4 were deposited (Fig. 11B). These seaward-connected channels will behave more like estuaries
561 and hence will receive, in part, a seaward-derived, landward-oriented sediment flux. Such units of
562 FA3 are likely to fine in a palaeolandwards direction, becoming more mud-rich as they approach
563 intertidal areas and/or gradually grading into narrower channel-shaped deposits of FA5. The
564 abundance of organic material in FA5 supports close proximity to a vegetated lower delta plain. This,
565 and the similar stratigraphic position to the distributary channels of FA4, suggests that the deposits
566 of FA5 were deposited in the lower delta plain. Inactive distributaries behave like estuaries, in which
567 flood-tidal currents can transport marine-derived sediment onshore (Dalrymple et al., 1992).

568 The second mechanism to explain the distribution of the mud-rich intervals results from the
569 development of a turbidity maximum zone. This model is often applied in other studies, but cannot
570 convincingly explain the observations made in the lower Sego Sandstone. The turbidity maximum
571 zone occurs where the suspension load of fresh water rivers mixes with saline waters, which can
572 result in clay flocculation. It has been hypothesized that in tide-dominated river deltas, the turbidity

maximum zone occurs further seaward than in estuaries, mainly because fluvial currents are stronger relative to tidal currents in river deltas compared to estuaries (Dalrymple & Choi, 2007). More sand-rich deposits are proposed to occur both landward and seaward of the turbidity maximum zone (Fig. 11C). Sand-rich deposits on the landward side of the turbidity maximum zone are dominated by offshore-directed fluvial currents. In contrast, sand-rich deposits on the seaward side are characterised by more bidirectional palaeocurrent patterns, in places dominated by onshore-directed, flood-tidal currents (Dalrymple & Choi, 2007). This partly resembles the distribution of mudstone that is present in the Sego Sandstone. Hence, cross-bedded sandstones (FA4) with onshore-directed palaeocurrents in interval S_1, which prograded over offshore mudstones and shoreface sandstones (FA1 and FA2), could represent deposits located seaward of the turbidity maximum zone. During continued progradation, relatively mudstone-rich deposits with bidirectional palaeocurrents (interval S_2) may represent deposition within the turbidity maximum zone. Subsequently, (interval S_3) cross-bedded sandstones (FA4) with offshore-directed palaeocurrents, could comprise fluvial-dominated distributary channels located landward of the turbidity maximum zone (Fig. 11C). The absence of cross-beds formed by dunes in FA3, which is most abundant in the relatively mudstone-rich interval S_2, is problematic for the interpretation of this interval as the preserved turbidity maximum zone, because such cross-beds were present in deposits (FA4) interpreted to form landward and seaward of the turbidity maximum zone, while it is expected that bedforms of uniform size are present along the axis of a single distributary channel (Dalrymple & Choi, 2007).

7.2. Analogues

The first depositional model outlined above, in which sandstones were deposited in active distributaries and relatively muddy deposits are more common in abandoned distributaries, is similar to inactive delta-plain regions of the present day Ganges-Brahmaputra and Mahakam river deltas (Fig. 11A). Both of these modern deltas are tide-influenced and contain regions with active distributaries separated by abandoned regions of the lower delta plain in which inactive distributary

599 channels have become estuaries (Allison et al., 2003; Storms et al., 2005; Salahuddin & Lambiase,
600 2013). The tide-dominated Fly and Yangtze river deltas are potential modern analogues for the
601 second depositional model, in which mud is deposited in the turbidity maximum zone (Fig. 11A).
602 Both the Fly and Yangtze deltas have an overall funnel shape, such that distributary channel
603 geometries and orientations are similar to those in tide-dominated estuaries. The analogy of the
604 lower Sego Sandstone with the Fly and Yangtze river deltas is another argument for the weakness of
605 the model in which the mud-rich facies are deposited in the turbidity maximum zone because the
606 modern analogues are situated in a confined setting, while the lower Sego Sandstone consists of two
607 sandstone tongues which extend seaward of their intervening coastline (Young, 1955; Willis & Gabel,
608 2003). The modern analogues cited above provide two end-member mechanisms to explain the
609 relative distributions of mudstone and sandstone in the lower Sego Sandstone. Both the Sego
610 Sandstone and the modern analogues are dominated by a grain size mix of mud and fine-grained
611 sand (Orton & Reading, 1993), so similar hydrodynamic conditions and geomorphologies are
612 expected. The modern analogues are all tide-dominated deltas developed under a tropical climate,
613 with high suspended sediment loads and containing mangrove-dominated flora, which facilitates
614 trapping of fine-grained sediment on the lower delta plain. In contrast, the lower Sego Sandstone
615 was deposited under a temperate climate with hot summers and cool winters (Sellwood & Valdes,
616 2006), is dominated by bedload-produced structures, and lacked salt-tolerant mangroves, which did
617 not evolve until the latest Cretaceous (Greb et al., 2006).

618 Another shortcoming of the Fly, Mahakam and Yangtze river delta analogues is the absence of
619 significant wave influence, which contrasts with the abundant storm-induced, HCS-bearing
620 sandstone beds in the delta front deposits of the lower Sego Sandstone (Van Wagoner, 1991; Willis
621 & Gabel, 2001; Legler et al., 2014). Consequently, the latter aspect of the “lower Sego Delta” has
622 been used to infer mixed tide and wave influence (e.g. Legler et al., 2014), rather than being tide-
623 dominated (cf. Willis & Gabel, 2001). Tide-dominated and wave-dominated areas can also coexist
624 laterally in modern deltas, such as in the modern Orinoco delta (Warne et al., 2002; Aslan et al.,

2003). Alternatively, deltas can also change their process character as they evolve with time. For example, tide- and/or fluvial-dominated deltas often characterise broad, shallow shelves, which can evolve into wave-influenced deltas as they prograde across narrow shelves towards deeper water (Yoshida et al., 2007; Ainsworth et al., 2008). Examples of the latter are the modern Mekong delta (Ta et al., 2002) and the Pliocene Orinoco delta (Chen et al., 2014; Bowman & Johnson, 2014). The "lower Sego Delta" can be interpreted in the light of this latter analogue. The higher abundance of wave-reworked facies in the more distal parts of the lower Sego Sandstone (Legler et al., 2014) suggests that storm-wave processes became gradually more dominant over time during progradation. In contrast, it can be argued that storm-wave produced facies (FA2) of the lower Sego Sandstone are preferentially preserved in more distal locations, below fairweather-wave base, and tide-influenced facies (FA3-5) in more proximal locations, above fairweather-wave base (Legler et al., 2014). The Niger delta has a similar distribution of depositional processes with a wave-dominated shoreline (Allen, 1964; Allen, 1965; Allen, 1970) and a tide-dominated lower delta plain where channel-fills and bars amalgamate laterally to form laterally continuous tide-dominated sand sheets (Oomkes, 1974). However, the distributary channels of the Niger are narrow, and hence, distinct mouth bars form at their mouths (Allen, 1964; Allen, 1965) while no mouth bar deposits are recognized in the lower Sego Sandstone. However, with the evidence currently available, it cannot be resolved whether the higher abundance of wave-dominated structures (FA2) in distal parts of the lower Sego Sandstone is the result of a temporal increase of wave-dominance or the preferential preservation of wave-dominated structures at the palaeo-coastline.

Figure 11B shows the envisioned depositional model for the lower Sego Sandstone, taking elements of the modern analogues which best fit the facies and architectural characteristics of the lower Sego Sandstone. The modern Niger and Mekong deltas form a good analogue for the distribution of a wave-dominated delta front and a tide-dominated lower delta plain. The Mahakam delta is taken as an analogue for the lateral distribution of active distributary channels and abandoned parts of the delta plain, where former distributary channels have become estuaries. The morphology of the river

mouths of the Mekong and Fly rivers can be taken as an analogue for the wide river mouths without fluvial mouth bars which are envisioned for the depositional model of the lower Sego Sandstone.

8. Conclusions

The lower Sego Sandstone is a net-regressive deltaic unit that exhibits mixed tide and wave influence. Deposits in the western (proximal) part of its outcrop belt, where fluvial and tidal processes interacted, have not been previously studied in detail, and consist of five facies associations. A complete idealized regressive succession consists of bioturbated mudstones containing planar, lenticular and wavy beds of siltstone and very fine-grained sandstone (FA1), which pass gradationally upwards into hummocky cross-stratified, very fine-grained sandstones (FA2), which in turn are overlain across a sharp-to-erosional surface by ripple cross-laminated and trough cross-bedded, sparsely bioturbated, fine-grained sandstones containing mudstone drapes (FA3, FA4). This succession is interpreted to record offshore deposits (FA1) overlain by storm-dominated, lower shoreface deposits on the distal delta front (FA2) and a tide-dominated facies-association complex on the proximal delta front and lower delta plain (FA3, FA4). Channelised mudstones and heterolithic mudstones (FA5) occurring towards the top of the lower Sego Sandstone are interpreted as abandoned distributary channel fills.

Up to four regressive successions are interpreted in the proximal, lower Sego sandstone (S_{-1}, S_0, S_1 and S_2-S_3, following and extending the nomenclature of earlier workers). The first and second successions (S_{-1}, S_0) each contain only offshore and distal delta front deposits (FA1, FA2), and are capped by offshore deposits (FA1) across an abandonment surface. These successions represent only the palaeoseaward parts of regressive tongues. The third succession (S_1) consists of offshore and lower shoreface deposits (FA1, FA2) and proximal delta front to lower delta plain deposits (FA4), in which palaeocurrents are directed predominantly onshore. Tide-dominated proximal delta front to lower delta plain deposits (FA4) are interpreted as the deposits of laterally migrating tidal bars that infilled shallow, low-relief channels in which flood tidal currents were dominant. The fourth

succession (S_2-S_3) contains only proximal delta front to lower delta plain deposits (FA3 and FA4), including a small proportion of channelised mudstones and muddy heterolithics that are interpreted to infill abandoned distributaries (FA5). Ripple cross-laminated, heterolithic sandstones (FA3) with a relatively high mudstone content and containing lenticular, wavy and flaser bedding with bidirectional palaeocurrent directions, are common in this succession. The upper part of this succession (S_3) comprises cross-bedded sandstones (FA4) with predominantly offshore-directed palaeocurrents that overlie high-relief channelised erosion surfaces, and which are interpreted as active distributary channels in which fluvial and/or ebb-tidal currents were dominant. Laterally extensive (>10 km) abandonment surfaces are absent in the tide-dominated deposits of the S_2-S_3 succession, and its subdivision is not straightforward.

The distribution of facies associations and mudstones in the proximal delta front to lower delta plain deposits (FA3, FA4, FA5) in the S_1, S_2 and S_3 intervals are explained by the avulsion and abandonment of active distributary channels. The relatively muddy strata of S_2 interval represent an abundance of abandoned distributary channels, which effectively became tide-dominated estuaries during abandonment, while the relatively sandy strata of the S_3 interval mainly contain the deposits of active fluvio-tidal distributaries and the S_1 interval of marine reworked sand. This model emphasises localised, autocyclic abandonment of parts of the delta, and is comparable to aspects of the modern Ganges-Brahmaputra and Mahakam river deltas.

Acknowledgments

Funding of fieldwork and approval for publication by Shell International and Shell Norway are gratefully acknowledged. We thank Julia Beckert, Renée de Bruijn, Dan Collins and Menno Hofstra for help in the field. We also thank Peter Allison, Jennifer Aschoff, Dan Collins, Berit Legler, Rodmar Ravnås, Ru Smith, Brian Willis and Lesli Wood for thought-provoking discussions of aspects of the work presented here. The insightful and constructive reviews of Brian Willis and an anonymous reviewer, and editorial comments of David Mohrig are gratefully acknowledged.

References

Ahnert, F. (1960) Estuarine Meanders in the Chesapeake Bay Area. *Geogr. Rev.,* **50**, 390-401.

Ainsworth, R.B., Flint, S.S. and Howell, J.A. (2008) Predicting coastal depositional style: Influence of basin morphology and accommodation to sediment supply ratio within a sequence stratigraphic framework. In: *Recent Advances in Models of Siliciclastic Shallow-Marine Stratigraphy* (Eds. G.J. Hampson, R.J. Steel, P.M. Burgess and R.W. Dalrymple), SEPM Sp. Publ. 90, 237-263.

Ainsworth, R.B., Vakarelov, B.K. and Nanson, R.A. (2011) Dynamic spatial and temporal prediction of changes in depositional processes on clastic shorelines: Toward improved subsurface uncertainty reduction and management. *AAPG Bull.,* **95**, 267-297.

Allen, G.P. and Chambers, J.L.C. (1998) Sedimentation in the modern and Miocene Mahakam Delta. Indonesian Petroleum Association, Jakarta, 236 pp.

Allen, J.R.L. (1964) The Nigerian continental margin: Bottom sediments, submarine morphology and geological evolution. *Mar. Geol.,* **1**, 289-332.

Allen, J.R.L. (1965) Late Quaternary Niger Delta, and Adjacent Areas: Sedimentary Environments and Lithofacies. *AAPG Bull.,* **49**, 547-600.

Allen, J.R.L. (1970) Sediments of the modern Niger Delta: A summery and review. In: *Deltaic Sedimentation, modern and ancient* (Ed. J.P. Morgan), SEPM Spec. Publ. 15, 138-151.

Allen, J.R.L. (1980) Sand waves: A model of origin and internal structure. *Sed. Geol.,* **26**, 281-328.

Allison, M.A., Khan, S.R., Goodbred Jr., S.L. and Kuehl, S.A. (2003) Stratigraphic evolution of the late Holocene Ganges–Brahmaputra lower delta plain. *Sed. Geol.,* **155**, 317-342.

Aschoff, J.L. and Steel, R.J. (2011a) Anatomy and development of a low-accommodation clastic wedge, upper Cretaceous, Cordilleran Foreland Basin, USA. *Sed. Geol.,* **236**, 1-24.

Aschoff, J.L. and Steel, R.J. (2011b) Anomalous clastic wedge development during the Sevier-Laramide transition, North American Cordilleran foreland basin, USA. *Geol. Soc. Am. Bull.,* **123**, 1822-1835.

Aslan, A., White, W.A., Warne, A.G. and Guevara, E.H. (2003) Holocene evolution of the western Orinoco Delta, Venezuela. *Geol. Soc. Am. Bull.,* **115**, 479-498.

Bhattacharya, J.P. and MacEachern, J.A. (2009) Hyperpycnal Rivers and Prodeltaic Shelves in the Cretaceous Seaway of North America. *J. Sed. Res.,* **79**, 184-209.

Blakey, R.C. (2013) North American Paleogeography, Late Cretaceous, Mid Campanian, ~77Ma (79-75). http://cpgeosystems.com/namkeypaleogeography.html.

Bowman, A.P. and Johnson, H.D. (2014) Storm-dominated shelf-edge delta successions in a high accommodation setting: The palaeo-Orinoco Delta (Mayaro Formation), Columbus Basin, South-East Trinidad. *Sedimentology,* **61**, 792-835.

Boyles, J.M. and Scott, A.J. (1982) A model for migrating shelf-bar sandstones in upper Mancos Shale (Campanian), northwestern Colorado. *AAPG Bull.,* **66**, 491-508.

Burton, D. and Wood, L.J. (2011) Quantitative shale characterization of the tidally influenced Sego Sandstone. *AAPG Bull.,* **95**, 1207-1226.

Chen, S., Steel, R.J., Dixon, J.F. and Osman, A. (2014) Facies and architecture of a tide-dominated segment of the Late Pliocene Orinoco Delta (Morne L'Enfer Formation) SW Trinidad. *Mar. Petrol. Geol.,* **57**, 208-232.

Choi, K.S., Dalrymple, R.W., Chun, S.S. and Kim, S. (2004) Sedimentology of Modern, Inclined Heterolithic Stratification (IHS) in the Macrotidal Han River Delta, Korea. *J. Sed. Res.,* **74**, 677-689.

Cobban, W.A.Walaszczyk, I.Obradovich, J.D. and McKinney, K.C.,(2006) A USGS Zonal Table for the Upper Cretaceous Middle Cenomanian-Maastrichtian of the Western Interior of the United States Based on Ammonites, Inoceramids, and Radiometric Ages. *US Geol. Surv. Open File Report,* **2006-1250**, 1-46.

Dalrymple, R.W., Knight, R.J., Zaitlin, B.A. and Middleton, G.V. (1990) Dynamics and facies model of a macrotidal sand-bar complex, Cobequid Bay-Salmon River estuary (Bay of Fundy). *Sedimentology,* **37**, 577-612.

Dalrymple, R.W. (1992) Tidal Depositional Systems. In: *Facies Models: Response to sea level change* (Eds. R.G. Walker and N.P. James), 195-218. Geological Association of Canada, St. John's.

Dalrymple, R.W., Zaitlin, B.A. and Boyd, R. (1992) Estuarine facies models; conceptual basis and stratigraphic implications. *J. Sed. Res.,* **62**, 1130-1146.

Dalrymple, R.W., Baker, E.K., Harris, P.T. and Hughes, M.G. (2003) Sedimentology and stratigraphy of a tide-dominated foreland-basin delta (Fly River, Papua New Guinea). In: *Tropical Deltas of Southeast Asia- Sedimentology, stratigraphy, and petroleum geology* (Eds. F. Hasan Sidi, D. Numedal, P. Imbert, H. Darman and H. Posamentier), SEPM Spec. Publ. 76, 147-173.

Dalrymple, R.W. (2006) Incised Valleys in Time and Space. In: *Incised Valleys in Time and Space* (Eds. R.W. Dalrymple, D.A. Leckie and R.W. Tillman), SEPM Spec. Publ. 85, 5-12.

Dalrymple, R.W. and Choi, K. (2007) Morphologic and facies trends through the fluvial–marine transition in tide-dominated depositional systems: A schematic framework for environmental and sequence-stratigraphic interpretation. *Earth-Sci.Rev.,* **81**, 135-174.

DeCelles, P.G. (2004) Late Jurassic to Eocene evolution of the Cordilleran thrust belt and foreland basin system, western U.S.A. *Am. J. Sci.,* **304**, 105-168.

Doelling, H.H.,(2002) Geologic map of the Moab and eastern part of the San Rafael Desert 30' X 60' quadrangles, Grand and Emery counties, Utah, and Mesa county Colorado. *Utah Geol. Surv.,* **1:100,000**.

Dott, R.H. and Bourgeois, J. (1982) Hummocky stratification: Significance of its variable bedding sequences. *Geol. Soc. Am. Bull.,* **93**, 663-680.

Dronkers, J. (1986) Tidal asymmetry and estuarine morphology. *Neth. J. Sea Res.,* **20**, 117-131.

Duke, W.L. (1985) Hummocky cross-stratification, tropical hurricanes, and intense winter storms. *Sedimentology,* **32**, 167-194.

Evans, G. (1965) Intertidal flat sediments and their environments of deposition in the Wash. *J. Geol. Soc.,* **121**, 209-240.

Fouch, T.D., Lawton, T.F., Nichols, D.J., Cashion, W.B. and Cobban, W.A. (1983) Patterns and timing of synorogenic sedimentation in Upper Cretaceous rocks of central and northeast Utah. In: *Mesozoic paleogeography of west-central United States* (Eds. M.W. Reynolds and E.D. Dolly), 305-336. Rocky Mountain Section, SEPM, Denver, Colorado.

Gaynor, G.C. and Swift, D.J.P. (1988) Shannon Sandstone depositional model; sand ridge dynamics on the Campanian Western Interior Shelf. *J. Sed. Petrol.,* **58**, 868-880.

Gill, J.R. & Hail, W.J.,(1975) Stratigraphic sections across Upper Cretaceous Mancos Shale-Mesaverde Group boundary, eastern Utah and western Colorado. *US Geol. Surv. Oil and Gas Inv. Chart,* **OC-68**.

Greb, S.F., DiMichele, W.A. and Gastaldo, R.A. (2006) Evolution and importance of wetlands in earth history. In: *Wetlands through time* (Eds. S.F. Greb and W.A. DiMichele), Geol. Soc. Am. Spec. Pap., 399, 1-40.

Gualtieri, J.L.,(2004) Geologic map of the Westwater 30' x 60' quadrangle, Grand and Uintah counties, Utah and Garfield and Mesa counties, Colorado. *US Geol. Surv.,* **1:100,000**.

Hampson, G.J. (2010) Sediment dispersal and quantitative stratigraphic architecture across an ancient shelf. *Sedimentology,* **57**, 96-141.

Hampson, G.J., Duller, R.A., Petter, A.L., Robinson, R.A.J. and Allen, P.A. (2014) Mass-Balance Constraints On Stratigraphic Interpretation of Linked Alluvial–Coastal–Shelfal Deposits From Source To Sink: Example From Cretaceous Western Interior Basin, Utah and Colorado, U.S.A. *J. Sed. Res.,* **84**, 935-960.

Harris, P.T., Pattiaratchi, C.B., Cole, A.R. and Keene, J.B. (1992) Evolution of subtidal sandbanks in Moreton Bay, eastern Australia. *Mar. Geol.,* **103**, 225-247.

Harris, P.T., Baker, E.K., Cole, A.R. and Short, S.A. (1993) A preliminary study of sedimentation in the tidally dominated Fly River Delta, Gulf of Papua. *Cont. Shelf Res.,* **13**, 441-472.

Harris, P.T. (1988) Large-scale bedforms as indicators of mutually evasive sand transport and the sequential infilling of wide-mouthed estuaries. *Sed. Geol.,* **57**, 273-298.

Harris, P.T., Hughes, M.G., Baker, E.K., Dalrymple, R.W. and Keene, J.B. (2004) Sediment transport in distributary channels and its export to the pro-deltaic environment in a tidally dominated delta: Fly River, Papua New Guinea. *Cont. Shelf Res.,* **24**, 2431-2454.

Hart, G.F., Pasley, M.A. and Gregory, W.A. (1994) Particulate organic matter, maceral facies models, and application to sequence stratigraphy. In: *Sedimentation of Organic Particles* (Ed. A. Traverse), 337-390. Cambridge University Press, New York.

Hasan Sidi, F., Nummedal, D., Imbert, P., Darman, H. and Posamentier, H.W. (2003) Tropical Deltas of Southeast Asia- Sedimentology, Stratigraphy, and Petroleum Geology. SEPM Spec. Publ. 76, 269 pp.

Hettinger, R.D. & Kirschbaum, M.A.,(2002) Stratigraphy of the Upper Cretaceous Mancos Shale (Upper Part) and Mesaverde Group in the Southern Part of the Uinta and Piceance Basins, Utah and Colorado. *US Geol. Surv. Geol. Inv.,* **I-2764**, 1-21.

Houbolt, J.J.H.C. (1968) Recent sediments in the southern bight of the North Sea. *Geol. Mijnbouw,* **47**, 245-273.

Hubbard, S.M., Smith, D.G., Nielsen, H., Leckie, D.A., Fustic, M., Spencer, R.J. and Bloom, L. (2011) Seismic geomorphology and sedimentology of a tidally influenced river deposit, Lower Cretaceous Athabasca Oil Sands, Alberta, Canada. *AAPG Bull.,* **95**, 1123-1145.

Johnson, M.A., Kenyon, N.H., Belderson, R.H. and Stride, A.H. (1982) Sand transport. In: *Offshore tidal sands* (Ed. A.H. Stride), 58-94. Chapman and Hall Ltd, London.

Keen, T.R., Slingerland, R.L., Bentley, S.J., Furukawa, Y., Teague, W.J. and Dykes, J.D. (2012) Sediment Transport on Continental Shelves: Storm Bed Formation and Preservation in Heterogeneous Sediments. In: *Sediments, Morphology and Sedimentary Processes on Continental Shelves: Advances in Technologies, Research, and Applications* (Eds. M.Z. Li, C.R. Sherwood and P.R. Hill), IAS Spec. Publ. 44, 295-310.

Kirschbaum, M.A. & Hettinger, R.D.,(2004) Facies Analysis and Sequence Stratigraphic Framework of Upper Campanian Strata (Neslen and Mount Garfield Formations, Bluecastle Tongue of the Castlegate Sandstone, and Mancos Shale), Eastern Book Cliffs, Colorado and Utah. *US Geol. Surv. Digital Data Ser.,* **DDS–69–G**, 1-40.

Legler, B., Johnson, H.D., Hampson, G.J., Massart, B.Y.G., Jackson, C.A., Jackson, M.D., El-Barkooky, A. and Ravnås, R. (2013) Facies model of a fine-grained, tide-dominated delta: Lower Dir Abu Lifa Member (Eocene), Western Desert, Egypt. *Sedimentology,* **60**, 1313-1356.

Legler, B., Hampson, G.J., Jackson, C.A., Johnson, H.D., Massart, B.Y.G., Sarginson, M. and Ravnås, R. (2014) Facies Relationships and Stratigraphic Architecture of Distal, Mixed Tide- and Wave-Influenced Deltaic Deposits: Lower Sego Sandstone, Western Colorado, U.S.A. *J. Sed. Res.,* **84**, 605-625.

Li, Y. and Bhattacharya, J. (2014) Facies architecture of asymmetrical branching distributary channels: Cretaceous Ferron Sandstone, Utah, USA. *Sedimentology,* **61**, 1452-1483.

Liu, S. and Nummedal, D. (2004) Late Cretaceous subsidence in Wyoming: Quantifying the dynamic component. *Geology,* **32**, 397-400.

Liu, S., Nummedal, D. and Gurnis, M. (2014) Dynamic versus flexural controls of Late Cretaceous Western Interior Basin, USA. *Earth Planet. Sci. Lett.,* **389**, 221-229.

MacEachern, J.A. and Bann, K.L. (2008) The Role of Ichnology in Refining Shallow Marine Facies Models. In: *Recent Advances in Models of Siliciclastic Shallow-Marine Stratigraphy* (Eds. G.J. Hampson, R.J. Steel, P.M. Burgess and R.W. Dalrymple), SEPM Spec. Publ. 90, 73-116.

Maguregui, J. and Tyler, N. (1991) Evolution of Middle Eocene tide-dominated deltaic sandstones, Lagunillas field, Maracaibo, western Venezuela. In: *The Three-Dimensional Facies Architecture of Terrigenous Clastic Sediments and Its Implications for Hydrocarbon Discovery and Recovery* (Eds. A.D. Miall and N. Tyler), 233-244. SEPM Concepts in Sedimentology and Paleontology Volume 3.

Martinius, A.W., Kaas, I., Næss, A., Helgesen, G., Kjærefjord, J.M. and Leith, D.A. (2001) Sedimentology of the heterolithic and tide-dominated Tilje Formation (Early Jurassic, Halten Terrace, Offshore Mid-Norway). In: *Sedimentary Environments Offshore Norway: Palaeozoic to Recent* (Eds. O.J. Martinsen and T. Dreyer), Norwegian Petroleum Society Spec. Publ. 10, 103-144.

McIlroy, D., Flint, S., Howell, J.A. and Timms, N. (2005) Sedimentology of the tide-dominated Jurassic Lajas Formation, Neuquén Basin, Argentina. In: *The Neuquen Basin, Argentina: A Case Study in Sequence Stratigraphy and Basin Dynamics* (Eds. G.D. Veiga, L.A. Spalletti, J.A. Howell and E. Schwarz), Geol. Soc. London Spec. Publ. 252, 83-107.

McLaurin, B.T. and Steel, R.J. (2000) Fourth-order nonmarine to marine sequences, middle Castlegate Formation, Book Cliffs, Utah. *Geology,* **28**, 359-362.

Mellere, D. and Steel, R. (2000) Style contrast between forced regressive and lowstand/transgressive wedges in the Campanian of south-central Wyoming (Hatfield Member of the Haystack Mountains Formation). In: *Sedimentary Responses to Forced Regressions* (Eds. D. Hunt and R.L. Gawthorpe), Geol. Soc. London Spec. Publ. 172, 141-162.

Nguyen, V.L., Ta, T.K.O. and Tateishi, M. (2000) Late Holocene depositional environments and coastal evolution of the Mekong River Delta, Southern Vietnam. *J. Asian Earth Sci.,* **18**, 427-439.

Oboh-Ikuenobe, F.E. (1996) Correlating palunofacies assemblages with sequence stratigraphy in Upper Cretaceous (Campanian) sedimentary rocks of the Book Cliffs, east-central Utah. *GSA Bull.,* **108**, 1275-1294.

Olariu, M.I., Olariu, C., Steel, R.J., Dalrymple, R.W. and Martinius, A.W. (2012) Anatomy of a laterally migrating tidal bar in front of a delta system: Esdolomada Member, Roda Formation, Tremp-Graus Basin, Spain. *Sedimentology,* **59**, 356-378.

Oomkes, E. and Terwindt, J.H.J. (1960) Inshore estuarine sediments in the Haringvliet (Netherlands). *Geol. Mijnbouw,* **39**, 701-710.

Oomkes, E. (1974) Lithofacies relations in the Late Quaternary Niger Delta complex. *Sedimentology,* **21**, 195-222.

Orton, G.J. and Reading, H.G. (1993) Variability of deltaic processes in terms of sediment supply, with particular emphasis on grain size. *Sedimentology,* **40**, 475-512.

Plink-Björklund, P. (2005) Stacked fluvial and tide-dominated estuarine deposits in high-frequency (fourth-order) sequences of the Eocene Central Basin, Spitsbergen. *Sedimentology,* **52**, 391-428.

Pontén, A. and Plink-Björklund, P. (2007) Depositional environments in an extensive tide-influenced delta plain, Middle Devonian Gauja Formation, Devonian Baltic Basin. *Sedimentology,* **54**, 969-1006.

Pontén, A. and Plink-Björklund, P. (2009) Process Regime Changes Across a Regressive to Transgressive Turnaround in a Shelf–Slope Basin, Eocene Central Basin of Spitsbergen. *J. Sed. Res.,* **79**, 2-23.

Posamentier, H.W. and Allen, G.P. (1999) Siliciclastic Sequence Stratigraphy - Concepts and Applications. SEPM Concepts in Sedimentology and Paleontology #7, 210 pp.

Posamentier, H.W. and Morris, W.R. (2000) Aspects of the stratal architecture of forced regressive deposits. In: *Sedimentary Responses to Forced Regressions* (Eds. D. Hunt and R.L. Gawthorpe), Geol. Soc. London Spec. Publ. 172, 19-46.

Prince, G.D. & Burgess, P.M.,(2013) Numerical Modeling of Falling-Stage Topset Aggradation: Implications for Distinguishing Between Forced and Unforced Regressions In the Geological Record. *J. Sed. Res.,* **83**, 767-781.

Reineck, H.E. (1967) Layered Sediments of Tidal Flats, Beaches, and Shelf Bottoms of the North Sea. In: *Estuaries* (Ed. G.H. Lauff), Am. Assoc. Adv. Sci. Spec. Publ. 83, 191-206, Stoudsburg.

Reineck, H.E. (1958) Longitudinale Schrägschicht im Watt. *Geol. Rundsch.,* **47**, 73-82.

Reineck, H.E. and Wunderlich, F. (1968) Classification and origin of flaser and lenticular bedding. *Sedimentology,* **11**, 99-104.

Salahuddin and Lambiase, J.J. (2013) Sediment Dynamics and Depositional Systems of the Mahakam Delta, Indonesia: Ongoing Delta Abandonment On A Tide-Dominated Coast. *J. Sed. Res.,* **83**, 503-521.

Seidler, L. and Steel, R. (2001) Pinch-out style and position of tidally influenced strata in a regressive-transgressive wave-dominated deltaic sandbody, Twentymile Sandstone, Mesaverde Group, NW Colorado. *Sedimentology,* **48**, 399-414.

Sellwood, B.W. and Valdes, P.J. (2006) Mesozoic climates: General circulation models and the rock record. *Sed. Geol.,* **190**, 269-287.

Sixsmith, P.J., Hampson, G.J., Gupta, S., Johnson, H.D. and Fofana, J.F. (2008) Facies architecture of a net transgressive sandstone reservoir analog: The Cretaceous Hosta Tongue, New Mexico. *AAPG Bull.,* **92**, 513-547.

Slingerland, R. and Keen, T.R. (1999) Sediment transport in the Western Interior Seaway of North America: Predictions from a climate-ocean-sediment model. In: *Isolated shallow marine sand bodies: Sequence stratigraphic analysis and sedimentologic interpretation* (Eds. K.M. Bergman and J.W. Snedden), SEPM Spec. Publ. 64, 179-190.

Sømme, T.O., Howell, J.A., Hampson, G.J. and Storms, J.E.A. (2008) Genesis, architecture, and numerical modelling of intra-parasequence discontinuity surfaces in wave-dominated deltaic deposits: Upper Cretaceous Sunnyside Member, Blackhawk Formation, Book Cliffs, Utah, U.S.A. In: *Recent Advances in Models of Siliciclastic Shallow-Marine Stratigraphy* (Eds. G.J. Hampson, R.J. Steel, P.M. Burgess and R.W. Dalrymple), SEPM Spec. Publ. 90, 421-441.

Staub, J.R. and Gastaldo, R.A. (2003) Late Quaternary sedimentation and peat development in the Rajang river delta, Sarawak, east Malaysia. In: *Tropical Deltas of Southeast Asia- Sedimentology,*

Stratigraphy, and Petreoleum Geology (Eds. F. Hasan Sidi, D. Nummedal, P. Imbert, H. Darman and H. Posamentier), SEPM Spec. Publ. 76, 71-78.

Steel, R.J., Plink-Björklund, P. and Aschoff, J.L. (2012) Tidal deposits of the Campanian Western Interior Seaway, Wyoming, Utah and Colorado, USA. In: *Principles of tidal sedimentology* (Eds. R.A. Davis and R.W. Dalrymple), 437-472. Springer, Dordrecht Heidelberg London New York.

Storms, J.E.A., Hoogendoorn, R.M., Dam, R.A.C., Hoitink, A.J.F. and Kroonenberg, S.B. (2005) Late-Holocene evolution of the Mahakam Delta, east Kalimantan, Indonesia. *Sed. Geol.,* **180**, 149-166.

Storms, J.E.A. and Hampson, G.J. (2005) Mechanisms for Forming Discontinuity Surfaces Within Shoreface–shelf Parasequences: Sea Level, Sediment Supply, or Wave Regime? *J. Sed. Res.,* **75**, 67-81.

Stukins, S., Jolley, D.W., McIlroy, D. and Hartley, A.J. (2013) Middle Jurassic vegetation dynamics from allochthonous palynological assemblages: An example from a marginal marine depositional setting; Lajas Formation, Neuquén Basin, Argentina. *Palaeogeogr., Palaeoclimatol., Palaeoecol.,* **392**, 117-127.

Ta, T.K.O., Nguyen, V.L., Tateishi, M., Kobayashi, I., Saito, Y. and Nakamura, T. (2002) Sediment facies and Late Holocene progradation of the Mekong River Delta in Bentre Province, southern Vietnam: an example of evolution from a tide-dominated to a tide- and wave-dominated delta. *Sed. Geol.,* **152**, 313-325.

Tänavsuu-Milkeviciene, K. and Plink-Björklund, P. (2009) Recognizing tide-dominated versus tide-influenced deltas; Middle Devonian strata of the Baltic Basin. *J. Sed. Res.,* **79**, 887-905.

Taylor, A.M. and Goldring, R. (1993) Description and analysis of bioturbation and ichnofabric. *J. Geol. Soc.,* **150**, 141-148.

Terwindt, J.H.J. (1971) Litho-facies of inshore estuarine and tidal-inlet deposits. *Geol. Mijnbouw,* **50**, 515-526.

Thomas, R.G., Smith, D.G., Wood, J.M., Visser, J., Calverley-Range, E.A. and Koster, E.H. (1987) Inclined heterolithic stratification—Terminology, description, interpretation and significance. *Sed. Geol.,* **53**, 123-179.

Tillman, R.W. and Martinsen, R.S. (1984) The Shannon shelf-ridge sandstone complex, Salt Creek anticline area, Powder River Basin, Wyoming. In: *Siliciclastic shelf sediments* (Eds. R.W. Tillman and C.T. Siemers), SEPM Spec. Publ. 34, 85-142.

Traverse, A., Ed. (1994) Sedimentation of Organic Particles. Cambridge University Press, Cambridge, 556 pp.

Trentesaux, A., Stolk, A. and Berné, S. (1999) Sedimentology and stratigraphy of a tidal sand bank in the southern North Sea. *Mar. Geol.,* **159**, 253-272.

Tyson, R.V. (1995) Sedimentary Organic Matter: organic facies and palynofacies. Chapman & Hall, London, 615 pp.

Van den Berg, J.H., Boersma, J.R. and Van Gelder, A. (2007) Diagnostic sedimentary structures of the fluvial-tidal transition zone - Evidence from deposits of the Rhine and Meuse. *Neth. J. Geosci.,* **86**, 387-306.

Van der Spek, A.J.F. (1997) Tidal asymmetry and long-term evolution of Holocene tidal basins in The Netherlands: simulation of palaeo-tides in the Schelde estuary. *Mar. Geol.,* **141**, 71-90.

Van Straaten, L.M.J.U. and Kuenen, P.H. (1957) Accumulation of fine grained sediments in the Dutch Wadden Sea. *Geol. Mijnbouw,* **19**, 329-354.

Van Straaten, L.M.J.U. (1961) Sedimentation in tidal flat areas. *J. Alberta Soc. Petrol. Geol.,* **9**, 203-213-46.

Van Veen, J., Van der Spek, A.J.F., Stive, M.J.F. and Zitman, T. (2005) Ebb and Flood Channel Systems in the Netherlands Tidal Waters. *J. Coast. Res.,* 1107-1120.

Van Wagoner, J.C. (1991) High-Frequency Sequence Stratigraphy and Facies Architecture of the Sego Sandstone in the Book Cliffs of Western Colorado and Eastern Utah. In: *Sequence Stratigraphy Applications to Shelf Sandstone Reservoirs* (Eds. J.C. Van Wagoner, C.R. Jones, D.R. Taylor, D. Nummedal, D.C. Jennette and G.W. Riley), AAPG Spec. Publ. 25, 15-42.

Visser, M.J. (1980) Neap-spring cycles reflected in Holocene subtidal large-scale bedform deposits: A preliminary note. *Geology,* **8**, 543-546.

Warne, A.G., Meade, R.H., White, W.A., Guevara, E.H., Gibeaut, J., Smyth, R.C., Aslan, A. and Tremblay, T. (2002) Regional controls on geomorphology, hydrology, and ecosystem integrity in the Orinoco Delta, Venezuela. *Geomorph.,* **44**, 273-307.

Willis, A. (2000) Tectonic control of nested sequence architecture in the Sego Sandstone, Neslen Formation and Upper Castlegate Sandstone (Upper Cretaceous), Sevier Foreland Basin, Utah, USA. *Sed. Geol.,* **136**, 277-317.

Willis, B.J., Bhattacharya, J.P., Gabel, S.L. and White, C.D. (1999) Architecture of a tide-influenced river delta in the Frontier Formation of central Wyoming, USA. *Sedimentology,* **46**, 667-688.

Willis, B.J. and Gabel, S.L. (2001) Sharp-based, tide-dominated deltas of the Sego Sandstone, Book Cliffs, Utah, USA. *Sedimentology,* **48**, 479-506.

Willis, B.J. and Gabel, S.L. (2003) Formation of Deep Incisions into Tide-Dominated River Deltas: Implications for the Stratigraphy of the Sego Sandstone, Book Cliffs, Utah, U.S.A. *J. Sed. Res.,* **73**, 246-263.

Witkind, I.J.,(2004) Geologic map of the Huntington 30' x 60' quadrangle, Carbon, Emery, Grand, and Uintah counties, Utah. *US Geol. Surv.,* **1:100,000**.

Wood, L.J. (2004) Predicting Tidal Sand Reservoir Architecture Using Data from Modern and Ancient Depositional Systems. In: *Integration of Outcrop and Modern Analogs in Reservoirs Modelling* (Eds. G.M. Grammer, P.M. Harris and G.P. Eberli), AAPG Mem., 80, 45-66.

Wright, L.D. (1977) Sediment transport and deposition at river mouths: A synthesis. *Geol. Soc. Am. Bull.,* **88**, 857-868.

Yang, C. and Nio, S. (1989) An ebb-tide delta depositional model—a comparison between the modern Eastern Scheldt tidal basin (southwest Netherlands) and the Lower Eocene Roda Sandstone in the southern Pyrenees (Spain). *Sed. Geol.,* **64**, 175-196.

Yoshida, S., Willis, A. and Miall, A.D. (1996) Tectonic control of nested sequence architecture in the Castlegate Sandstone (Upper Cretaceous), Book Cliffs, Utah. *J. Sed. Res.,* **66**, 737-748.

Yoshida, S., Jackson, M.D., Johnson, H.D., Muggeridge, A.H. and Martinius, A.W. (2001) Outcrop studies of tidal sandstones for reservoir characterization (Lower Cretaceous Vectis Formation, Isle of Wight, Southern England). In: *Sedimentary Environments Offshore Norway - Palaeozoic to Recent* (Eds. O.J. Martinsen and T. Dreyer), Norwegian Petroleum Society Spec. Publ. 10, 233-257.

Yoshida, S., Johnson, H.D., Pye, K. and Dixon, R.J. (2004) Transgressive changes from tidal estuarine to marine embayment depositional systems: The Lower Cretaceous Woburn Sands of southern England and comparison with Holocene analogs. *AAPG Bull.,* **88**, 1433-1460.

Yoshida, S., Steel, R.J. and Dalrymple, R.W. (2007) Changes in Depositional Processes—An Ingredient in a New Generation of Sequence-Stratigraphic Models. *J. Sed. Res.,* **77**, 447-460.

Young, R.G. (1955) Sedimentary facies and intertonguing in the Upper Cretaceous of the Book Cliffs, Utah-Colorado. *Geol. Soc. Am. Bull.,* **66**, 177-202.

Zhuo, H., Wang, Y., Shi, H., Zhu, M., He, M., Chen, W. and Li, H. (2014) Seismic geomorphology, architecture and genesis of Miocene shelf sand ridges in the Pearl River Mouth Basin, northern South China Sea. *Mar. Petrol. Geol.,* **54**, 106-122.

1012 Table and Figure captions

FA#	FA Name	Lithology	Primary sedimentary structures	Biogenic structures	Geometry	Dimensions	Interpretation
1	Bioturbated mudstones	Mudstones, siltstones and very fine-grained sandstones	Siltstone and very fine grained sandstone beds (<10 cm thick) with sharp bases and sharp and gradational tops, internally low angle cross-lamination.	BI=0-4. *Palaeophycus*, *Planolites*, *Schaubcylindrichnus*, *Thalassinoides*, *Skolithos*, *Arenicolites*.	Tabular	5 to 10 m thick x over 25 km wide	Offshore mudstones
2	Humocky cross stratified sandstones	Very fine- and fine-grained sandstones and mudstones	Hummocky cross stratification in sharp-based sandstone beds that are variably amalgamated.	BI=0-2. *Skolithos*, *Palaeophycus*, *Ophiomorpha*, *Planolites*, *Arenicolites*, *Diplocraterion*.	Tabular	2 to 10 m thick x 10 to over 25 km wide	Lower shoreface
3	Ripple cross-laminated heterolithic sandstones	Very fine- and fine-grained sandstones and mudstones	Lenticular, wavy and flaser bedding. Wave ripples and current ripples. Bidirectional palaeocurrent directions.	BI=0-2. *Ophiomorpha*, *Thalassinoides*, *Skolithos*, *Planolites*, *Palaeophycus*, *Gyrochorte*.	Tabular	0 to 4 m thick x 1 to 8 km wide	Coarsening upward tidal bar
4	Cross-bedded sandstones	Fine- to medium-grained sandstones and mudstones	Sets of cross-beds with mudstone-draped foresets and rippled toesets.	BI=0-2. *Ophiomorpha*, *Skolithos*, *Palaeophycus*, *Planolites*, *Gyrochorte*, *Arenicolites*, *Rosellia*, *Cylindrichnus*, *Teredolites*.	Tabular or lenticular	Tabular: 1 to 10 m thick x 1 to over 25 km wide; Lenticular: 1 to 15 m thick x 300 m wide x 2 to 4 km long	Inter-channel tidal bars and tidal channel fills
5	Sharp-based mudstones and heterolithic mudstones	Mudstones and very fine-grained sandstones	Lenticular and wavy bedding. Rich in organic matter.	BI=0-1. *Planolites*.	Lenticular	0.5 to 5 m thick x 0.5 to 2 km wide	Abandoned distributary channels

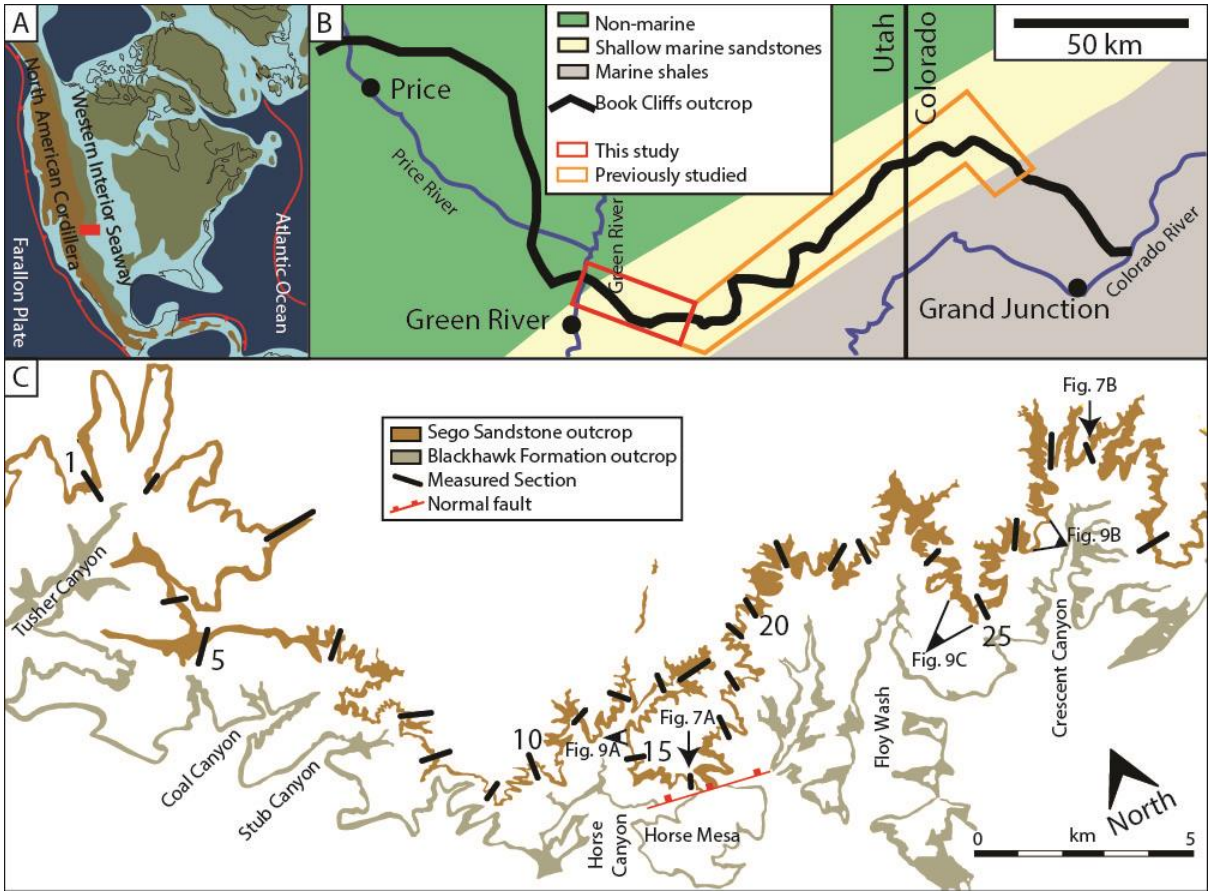
1013 **Table 1.** Summary of facies associations.

1014

Sample number	FA#	Trilete Spores	Bisaccate Pollen	Other Pollen	Dinoflagellates	Resin	Opaque-Equidimensional	Opaque-Bladed	Translucent	Cuticle	Amorphous organic matter	Prasinophytes
FA1-1	1	2.45	0.35	1.4	0	2.8	13.64	6.29	67.83	5.24	0	0
FA1-2	1	0.98	0.33	0.98	0	1.97	8.85	11.48	74.43	0.98	0	0
FA3-1	3	0	0	0.32	0	1.28	31.95	8.31	45.37	12.14	0.64	0
FA3-2	3	0.31	0	0	0	3.76	26.33	8.46	49.53	11.6	0	0
FA3-3	3	2.01	1.34	0	1.01	3.02	7.05	7.72	70.47	7.05	0.34	0
FA3-4	3	0.32	0.00	0.95	0.32	2.53	6.96	7.28	75.95	5.38	0	0.32
FA5-1	5	0.64	0.64	0.96	0.32	1.92	7.67	5.11	73.8	6.71	2.25	0

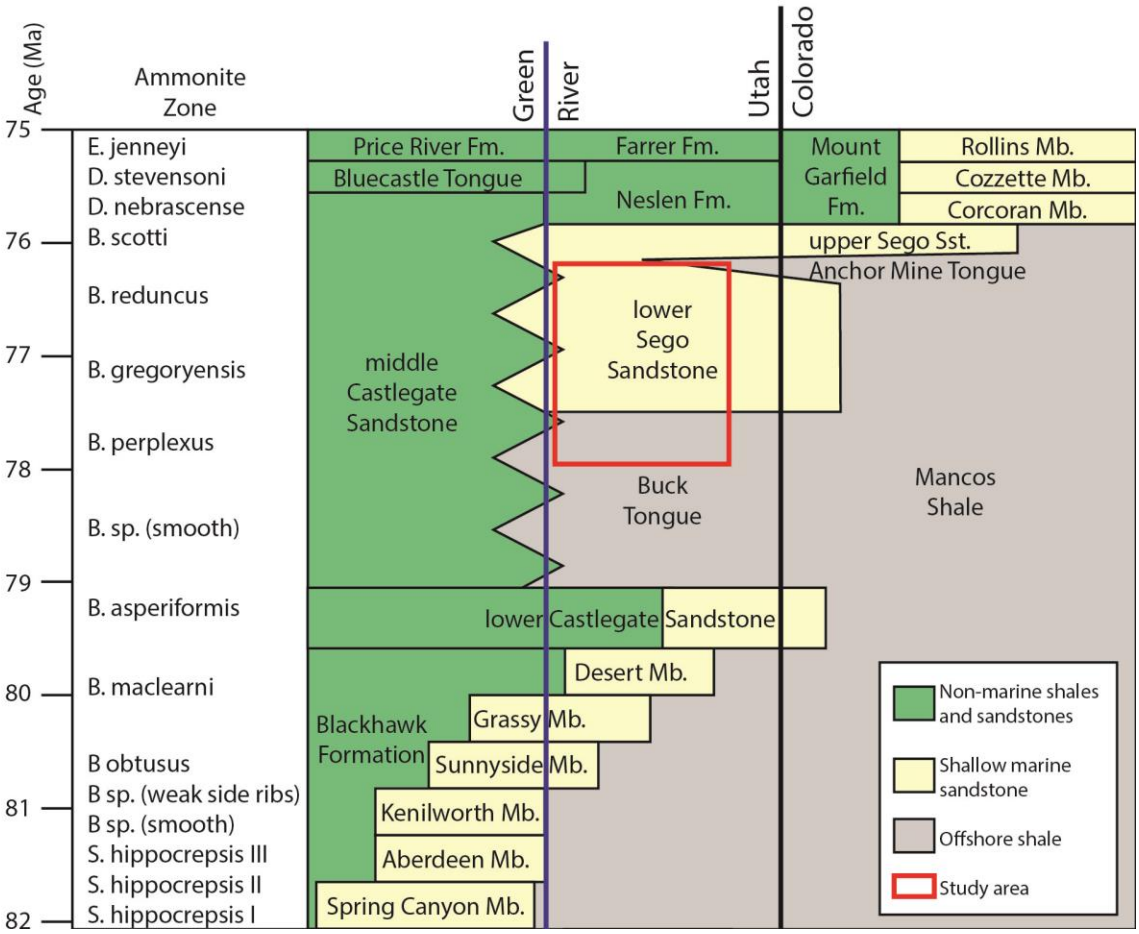
1015 Table 2: Sample percentage of palynofacies counts.

1016



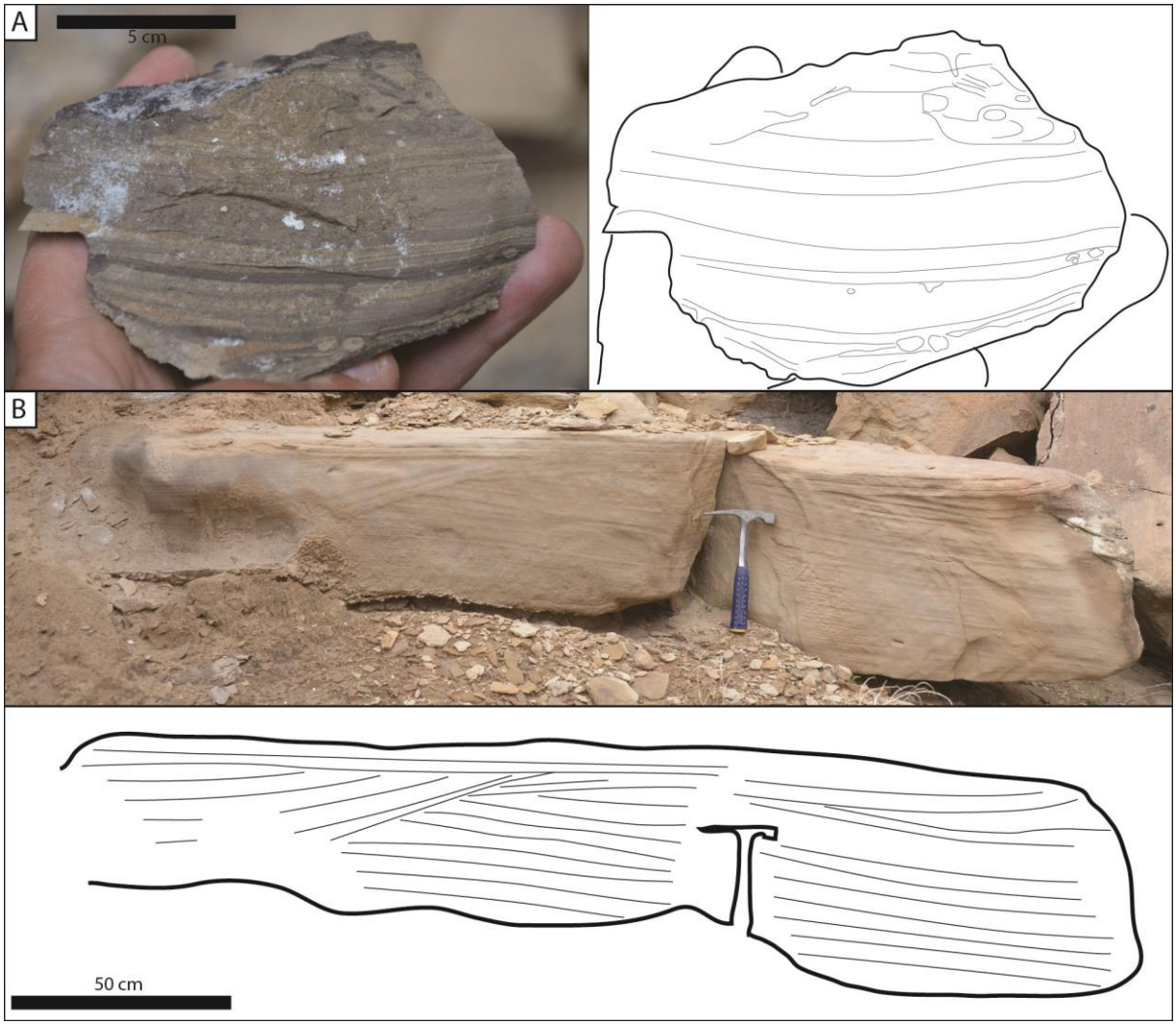
1017

1018 **Fig. 1.** (A) Palaeogeographic reconstruction of the North American continent during the Campanian.
1019 The black lines indicate modern coastline positions. The Sego Sandstone outcrop belt (Fig. 1B) is
1020 indicated by the red box (modified after Blakey, 2013). (B) Map showing the study area in the
1021 context of the Sego Sandstone outcrop belt in the Book Cliffs and the gross interpreted
1022 palaeogeography of the unit (modified after Willis & Gabel, 2001). (C) Map of the study area
1023 showing the Sego Sandstone, and the location of stratigraphic logs and photo panoramas discussed
1024 in this paper (modified after Doelling, 2002; Gualtieri, 2004; Witkind, 2004).



1025

1026 **Fig. 2.** Lithostratigraphy of the Sego Sandstone and neighbouring units. The red box indicates the
1027 studied interval (modified after Young, 1955; Gill & Hail, 1975; Fouch et al., 1983; McLaurin & Steel,
1028 2000; Kirschbaum & Hettinger, 2004; Cobban et al., 2006).



1029

1030 **Fig. 3.** Facies associations 1 and 2. (A) Mudstone with thin siltstone beds and sparse bioturbation by

1031 *planolites* (FA1). (B) Very fine-grained sandstone bed containing HCS (FA2).

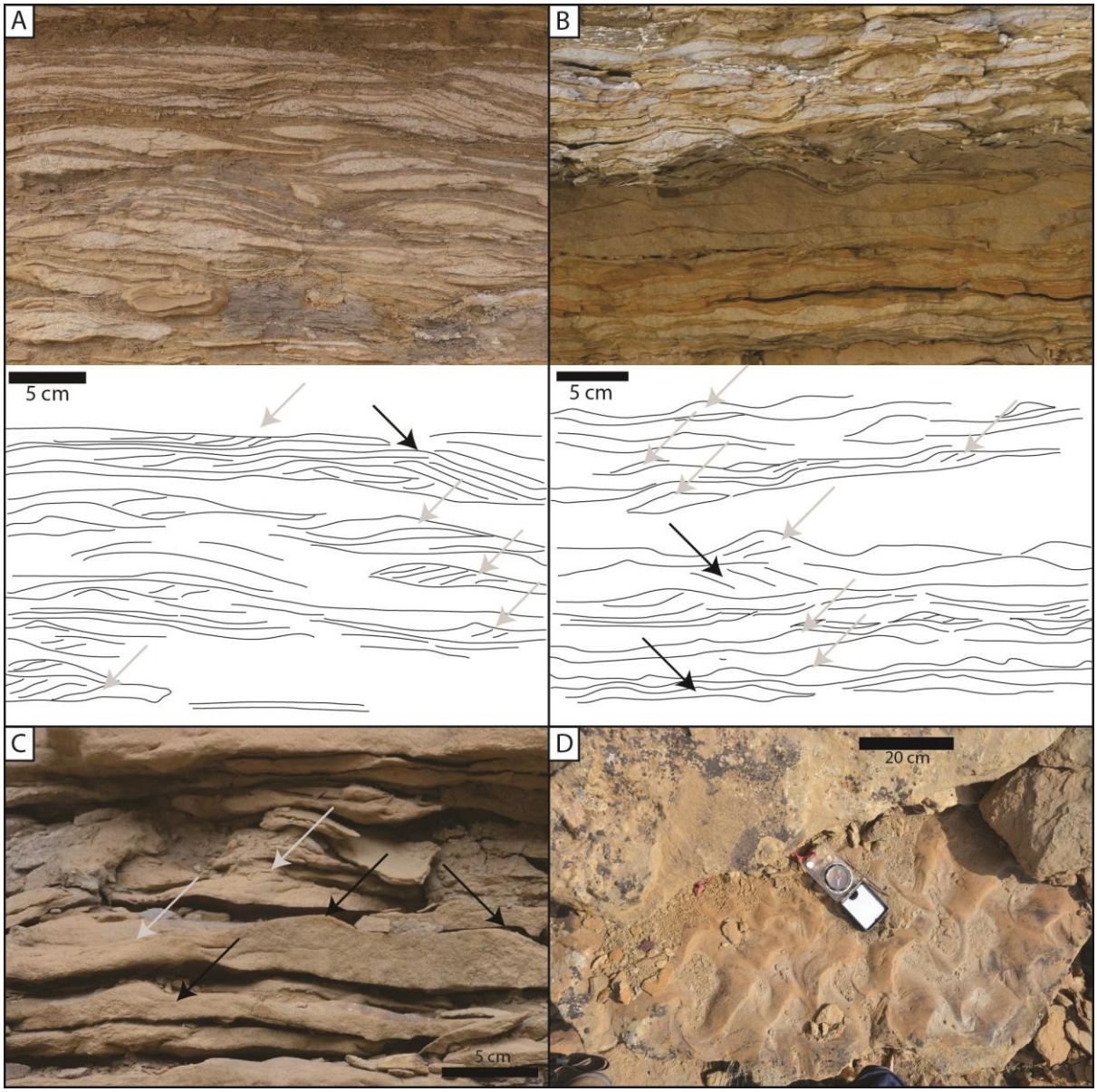


Fig. 4. Facies association 3. (A) (B) and (C) Current rippled and cross-laminated heterolithic sandstones exhibiting apparent bidirectional palaeocurrents. The black and grey arrows indicate cross lamination and current ripples of apparent opposed palaeoflow directions. (D) Three dimensional current ripples indicating palaeoflow towards the SE.

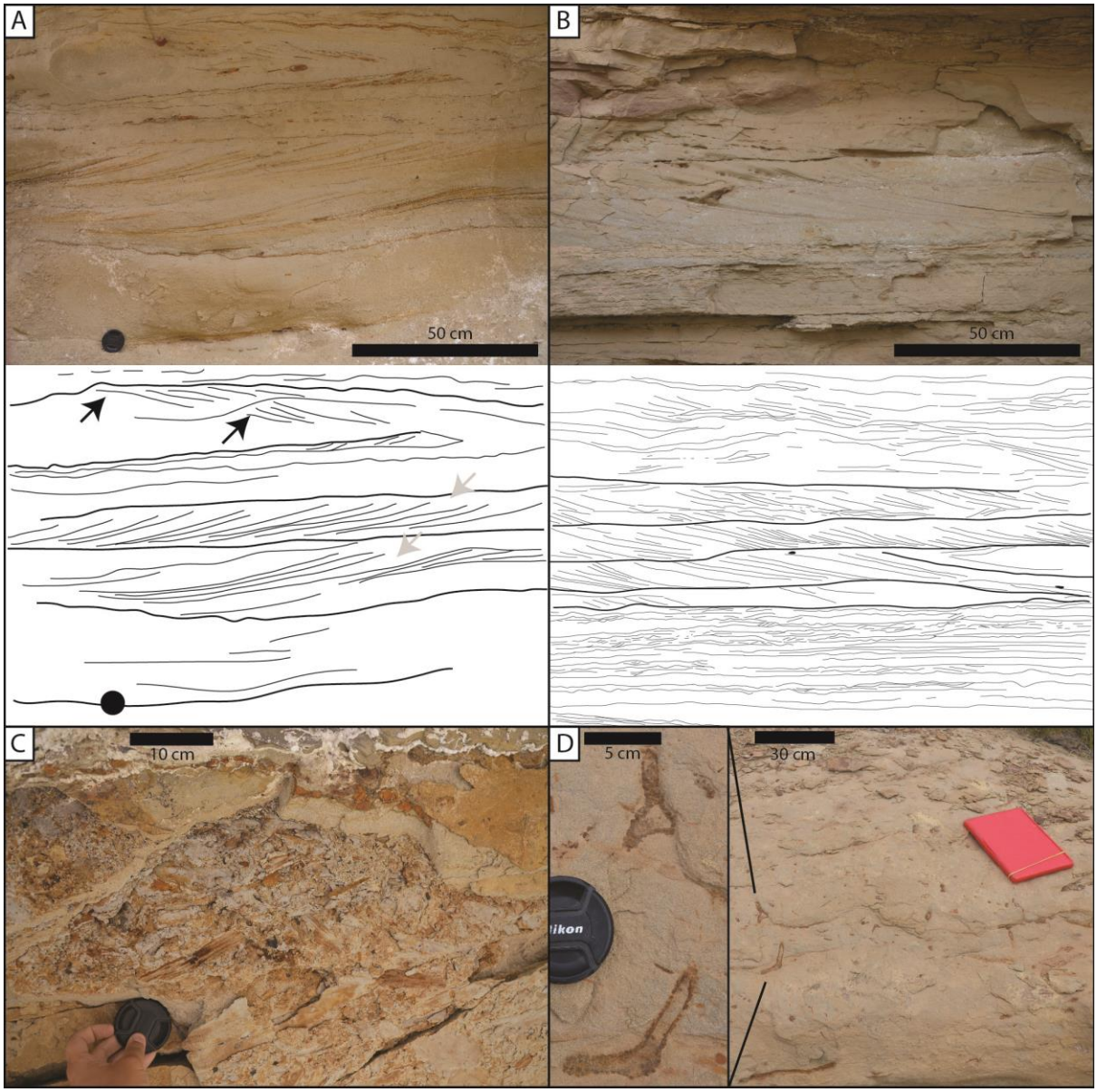


Fig. 5. Facies association 4. (A) and (B) Mud draped, cross-bedded heterolithic sandstones of FA4. Palaeocurrents are unidirectional except for the top beds in (A) which show an opposed apparent palaeoflow directions (grey and black arrows). Toesets consist of cross-laminated wavy and lenticular bedding. In (A) mudclasts are randomly scattered and aligned along bed bases and foresets. (C) Lag of mudstone clasts and wood debris at the erosional base of a unit of FA4. (D) Bioturbation by *Ophiomorpha* at the top of a bed in FA4.

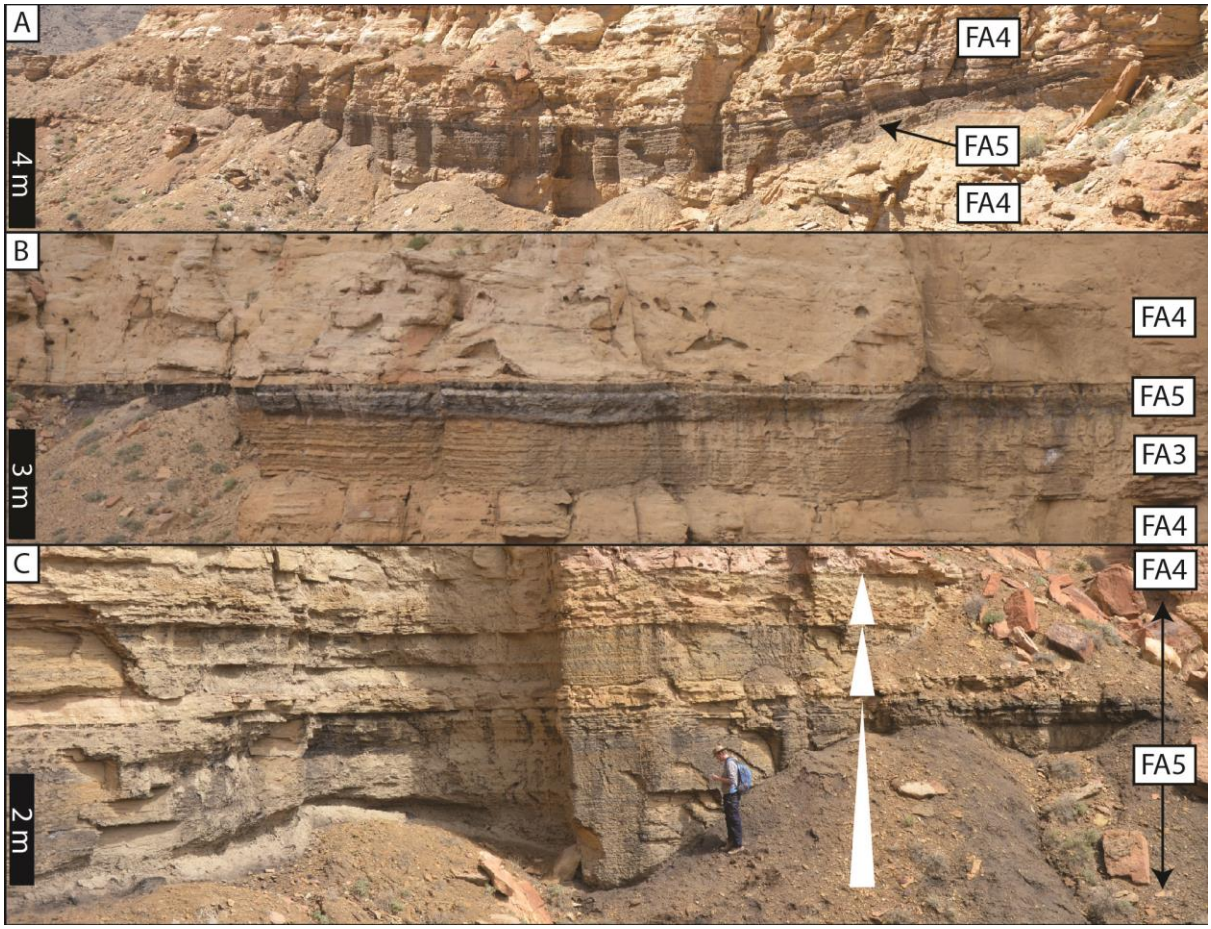
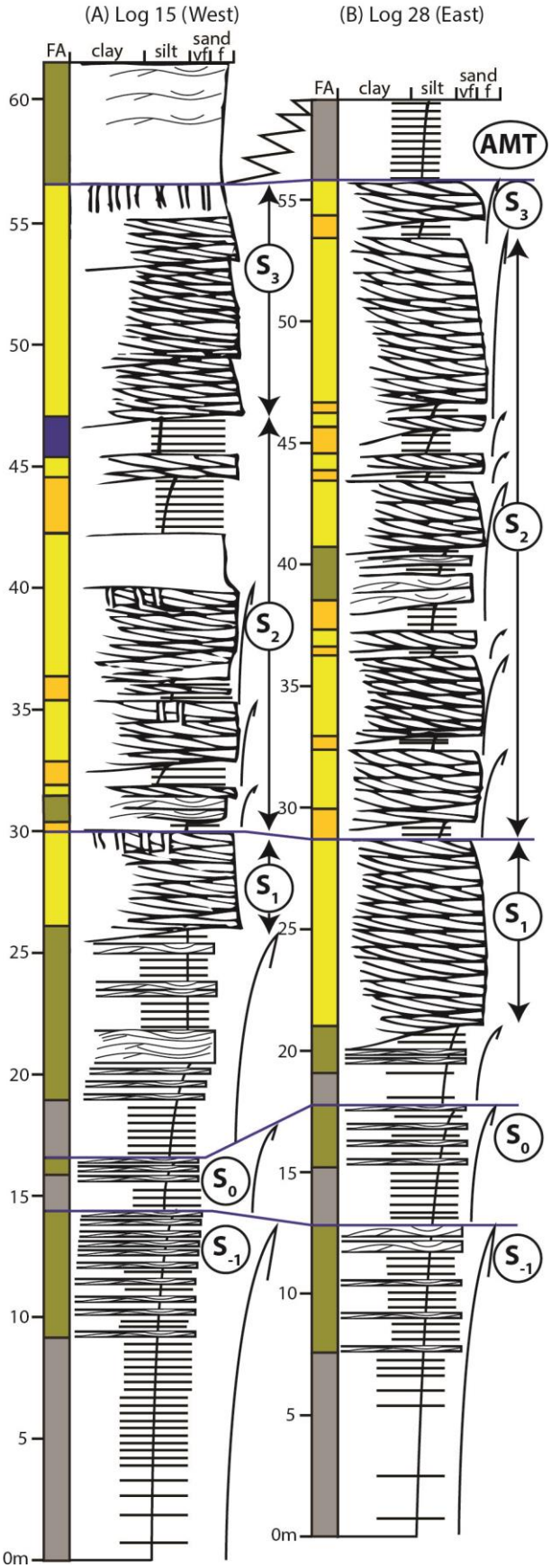
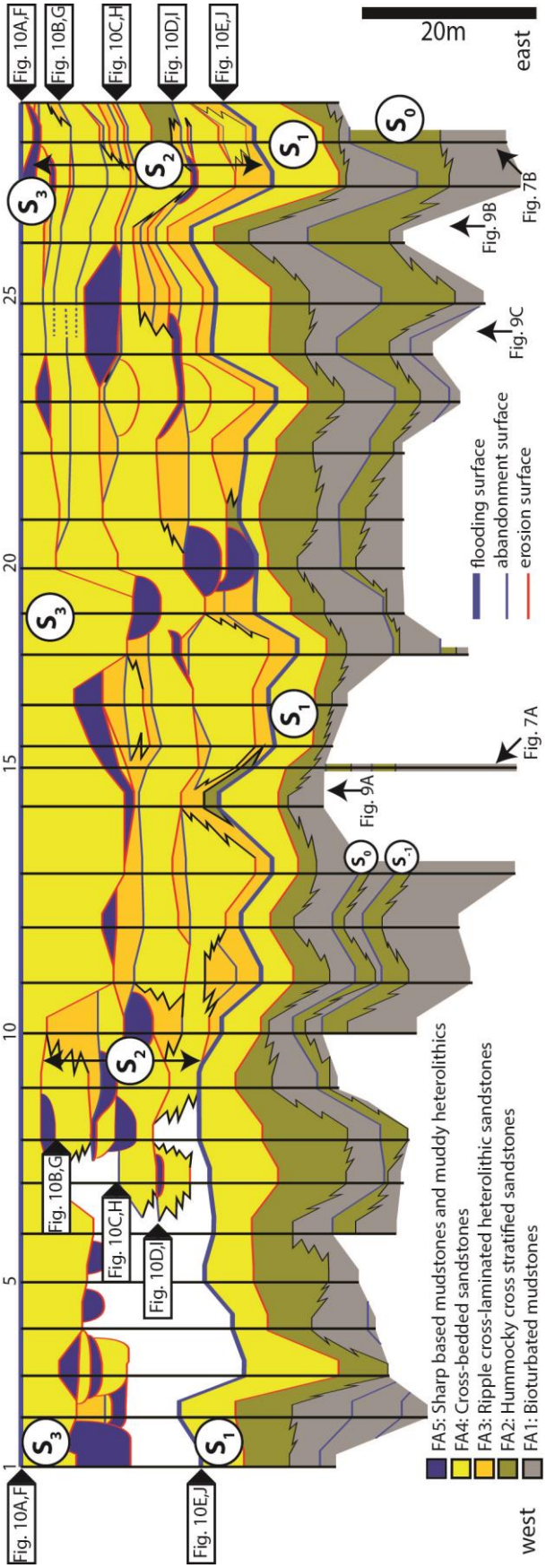


Fig. 6. Facies association 5. (A) Lenticular channel fill of FA5 that erosionally truncates deposits of FA4. Mudstones drape the concave-up base of the channel and are themselves truncated by an overlying channel-fill sandstone of FA4. (B) Organic-rich mudstones of FA5 that truncate underlying rippled heterolithic sandstones (FA3) and which are erosionally overlain by cross-bedded sandstones (FA4). (C) Stacked mudstone channel fills of FA5. Individual channel fills fine upward and their erosional bases are marked by sharp increases in grain size. Triangles mark grain size trends within each channel fill.


(A) Log 15 (West)
(B) Log 28 (East)
FA
clay
silt
sand
vf
f
AMT
S3
S2
S1
S0
S-1
60
55
50
45
40
35
30
25
20
15
10
5
0m

1052

1053 **Fig. 7.** Representative stratigraphic logs showing vertical facies successions through the lower Sego
1054 Sandstone in the western (A) and eastern (B) parts of the study area (Figs. 1C, 8). Correlative
1055 surfaces that can be traced across the study area are shown between the two logs, and delimit
1056 upward-coarsening successions (named according to the nomenclature of Willis & Gabel, 2001;
1057 names are encircled). The base of the Anchor Mine Tongue (AMT) at the top of the lower Sego
1058 Sandstone is used as a datum. The arrows indicate grain size trends. For explanation of the colours
1059 representing the facies associations (FA), see Figure 8.


Fig. 10A,F
Fig. 10B,G
Fig. 10C,H
Fig. 10D,I
Fig. 10E,J
20m
east
west
1
5
10
15
20
25
S_0
S_1
S_2
S_3
S_{-1}
Fig. 9A
Fig. 9B
Fig. 9C
Fig. 7A
Fig. 7B
flooding surface
abandonment surface
erosion surface
FA5: Sharp based mudstones and muddy heterolithics
FA4: Cross-bedded sandstones
FA3: Ripple cross-laminated heterolithic sandstones
FA2: Hummocky cross stratified sandstones
FA1: Bioturbated mudstones

1060

1061 **Fig. 8.** Correlation panel through stratigraphic logs in the study area, from west (palaeolandward) to
1062 east (palaeoseaward) (Fig. 1B, C), showing detailed facies architecture in the lower Sego Sandstone.
1063 The base of the Anchor Mine Tongue and coincident top of the lower Sego Sandstone (Fig. 2) is used
1064 as a datum. Key stratigraphic surfaces that have been mapped over the study area, or whose
1065 correlation is inferred, are shown. See text for details.

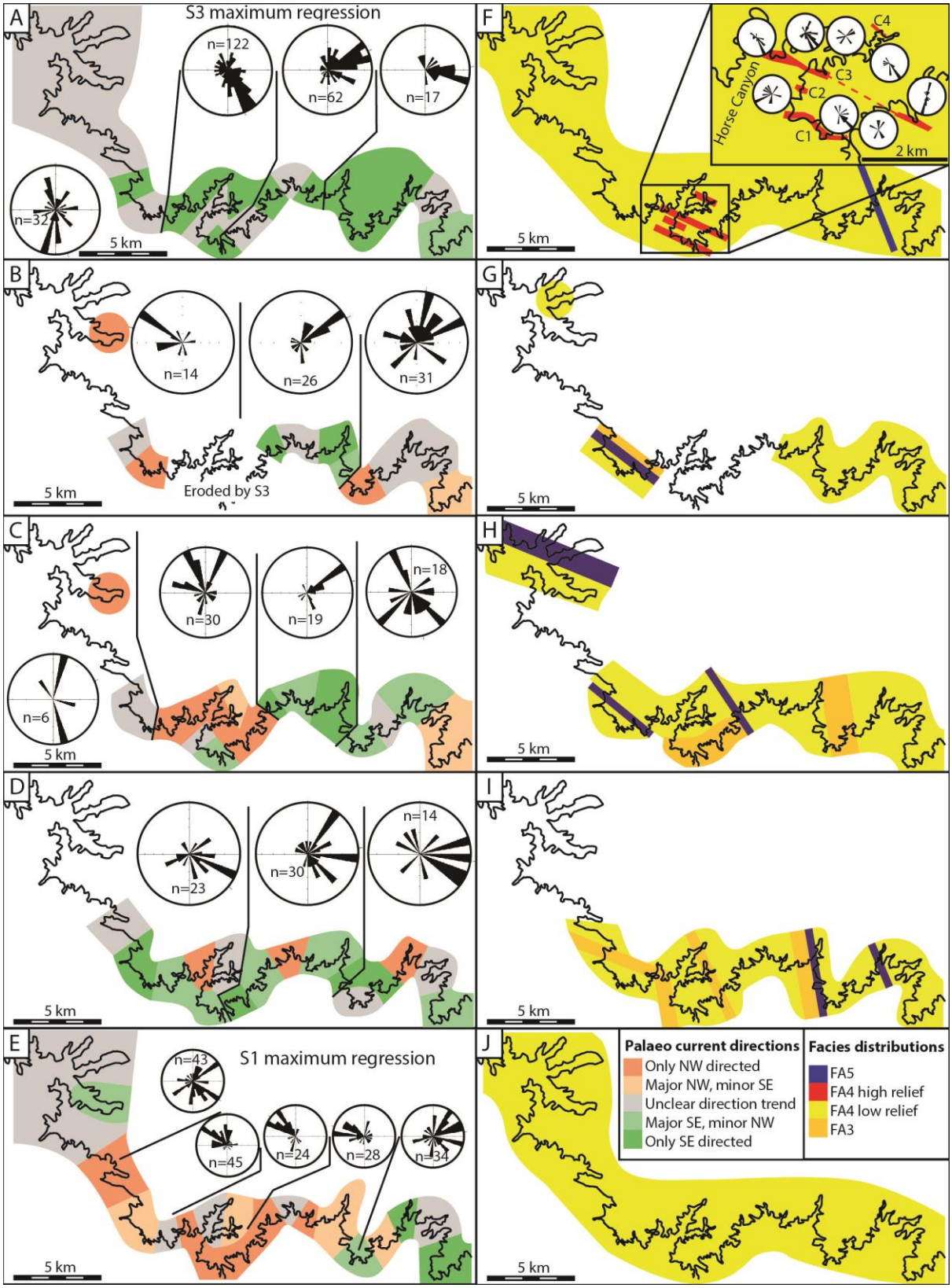


1066

1067 **Fig. 9.** Uninterpreted photo-panoramas (top) and interpreted line drawings (bottom) of selected

1068 stratigraphic architectures and facies distributions exposed in cliff-face amphitheatres (located in

1069 Figs. 1C, 8). (A) High-relief erosional surface at the base of succession S_3. On the left (north), the
1070 erosional surface cuts out a channelised mudstone (FA5). (B) Facies architecture in the eastern part
1071 of the study area. Erosion surfaces at the base of cross-bedded sandstones (FA4) in successions S_1, S_2
1072 and S_3 have low relief, and there are lateral changes in sandstone content (between FA3 and FA4)
1073 within succession S_2. (C) Thick channelised mudstone on the left (white arrows) and inclined surfaces
1074 in the prominent sandstone of FA4 in S_2 (black arrows).



1075

1076 **Fig. 10.** Maps of (A-E) palaeocurrent distributions and (F-J) facies-association distributions for five

1077 stratigraphic levels (Fig. 8): (A, F) maximum regression in succession S_3; (B, G) upper part of

succession S_2; (C, H) middle part of succession S_2; (D, I) lower part of succession S_2; and (E, J) maximum regression in succession S_1. Red lines in (F) indicate the axes of high-relief channelised erosion surfaces filled with cross-bedded sandstones (FA4) in succession S_3 (e.g. Fig. 9A). The inset in (F) shows a detailed map of the Horse Mesa area.

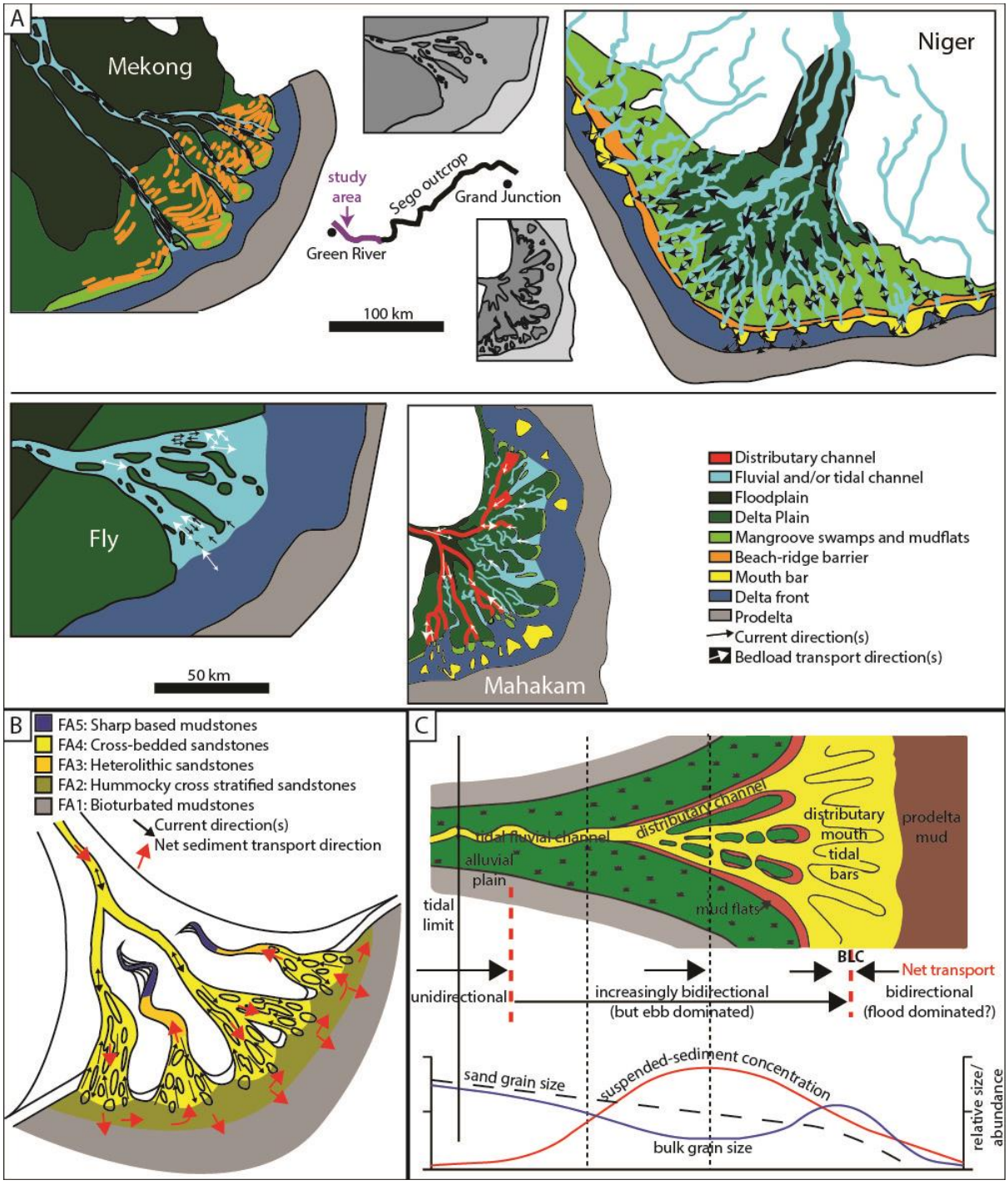


Fig. 11. (A) The morphologies of selected modern analogues for the lower Sego Sandstone discussed in the text: the Niger (Allen, 1965; Allen, 1970), Mekong (Nguyen et al., 2000), Mahakam (Allen & Chambers, 1998; Salahuddin & Lambiase, 2013) and Fly River (Dalrymple et al., 2003; Harris et al., 2004) deltas. The outline of the Sego Sandstone outcrop belt is shown at the same scale as detailed maps of the Niger and Mekong deltas, while the Fly and Mahakam deltas are shown in outline at the same scale (black and white) and are enlarged in detailed maps. (B) Proposed model for the lower Sego Sandstone. Active distributaries show a downstream increase in (flood) tidal influence. Abandoned distributaries become estuaries and show a landward fining trend. See text for further discussion. (C) Conceptual model for the distribution of facies in tide-dominated deltas based in part on the Fly River delta (modified after Dalrymple & Choi, 2007).